24(2)

24(2)

気象庁欧文海洋報告

LIBRARY

第24巻 第2号

DEC 2 1974

FISH & WILDLIFE SERVICE

THE OCEANOGRAPHICAL MAGAZINE

Vol. 24 No. 2

CONTENTS

AKAGAWA, M.: The characters of atmospheric circulation in the years with abnormal sea ice conditions along the Okhotsk coast of Hokkaido, Japan 81

DEN, N. and M. YASUI: A note on the palaeogeographic location of trenches ..101

ISEZAKI, N.: Geomagnetic anomalies and tectonics around the Japanese Islands 107

Published by the Japan Meteorological Agency

March, 1973

Digitized by the Internet Archive
in 2025

https://archive.org/details/oceanographical-magazine_1973-03_24_2

The Oceanographical Magazine
Vol. 24, No. 2, pp. 81 to 100, March 1973

The characters of atmospheric circulation in the years with abnormal sea ice conditions along the Okhotsk coast of Hokkaido, Japan

Masaomi AKAGAWA

Hakodate Marine Observatory

(Received 4 December 1972)

Abstract: Analysis of the historical series (1946–1972) of the dates of pack ice appearance and disappearance at the Okhotsk coast of Hokkaido, Japan is made. The years when the departures of those dates of pack ice appearance or disappearance from the normals are equal to or exceeding the standard deviations are defined as the abnormal years.

The characters of atmospheric circulation in the preceding December and November for the abnormal years on the date of pack ice appearance and in March for the abnormal years on the date of pack ice disappearance are investigated.

It is seen that there are remarkable contrasts between markedly early years and markedly late years of the dates of pack ice appearance and disappearance, respectively, in regard to the features of sea level atmospheric pressure and 500-mb height patterns, and the zonal or meridional flow on the 500-mb surface.

Features of air temperature anomaly distribution are also noted.

1. Introduction

Along the Okhotsk coast of Hokkaido, Japan, the average date of pack ice appearance is 16th January, arithmetic mean of the values at Kitamiesashi, Omu, Mombetsu and Abashiri from 1946 to 1972, and the standard deviation is 9 days; on the other hand the average date of pack ice disappearance is 1st April, arithmetic mean of the values at Kitamiesashi, Omu and Mombetsu, and the average date at Abashiri is 18th April, and the standard deviations are 16 days for the stations.

The location of each station is shown in Fig. 1. Generally speaking, drift of pack ice and expansion or reduction of ice area are controlled by wind, ocean current, air temperature and water temperature. It is acceptable, however, that wind plays the most important role in variation of ice conditions, considering changeability of wind, attribution of air temperature to wind system and weak effect of ocean current in the Okhotsk Sea. Therefore, atmospheric circulation is thought to be the problem for discussion.

Previously the problems of relations between atmospheric circulation and sea ice conditions were discussed in the light of long-range sea ice forecasting and climatology by several authors (WIESE, 1924; CHISHIMA, 1962; SCHELL, 1964; AKAGAWA, 1967; STRÜBING, 1967; BERGTHÓRSSON, 1970; SANDERSON, 1971; RODEWALD, 1971; and scientists of U.S.S.R. [See reference of KUSUNOKI (1955) and ARMSTRONG (1955)]. In this paper the character of atmospheric circulation in the years of abnormal sea ice conditions on the Okhotsk coast of Hokkaido is studied.

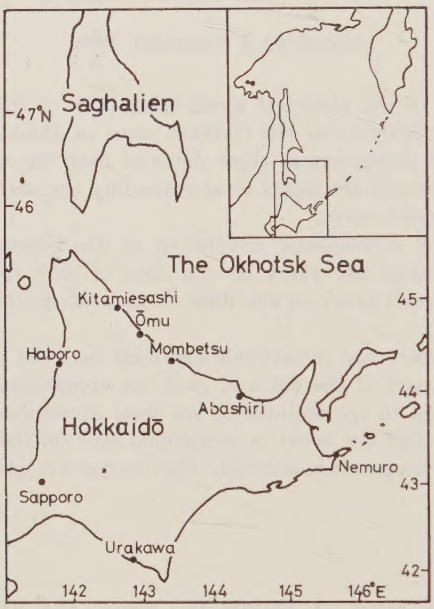

Fig. 1. Location of stations.

2. Statistics of the dates of pack ice appearance and disappearance

As seen in Fig. 2, the differences of the dates of pack ice appearance among the stations are small, but the dates of pack ice disappearance fluctuate relatively and ranges of inter-annual variations are also large. This difference seems to be due to the following facts: in the season when pack ice appears (December～January) the wind system is stable because the winter monsoon blows, and pack ice field is condensed. On the other hand, in the season when pack ice disappears (March～April) the wind system is unstable because it comes under a transitional period from winter to spring, and pack ice field becomes loose. Therefore arrangement and motion processes of pack ice are made rapidly and are not uniform regionally

Fig. 3 shows the histogram of the date of pack ice appearance at Abashiri (1892–1972) and that of the dates of pack ice disappearance at Abashiri (1892–1972) and Kitamiesashi (1943–1972). The earliest date of pack ice appearance at Abashiri

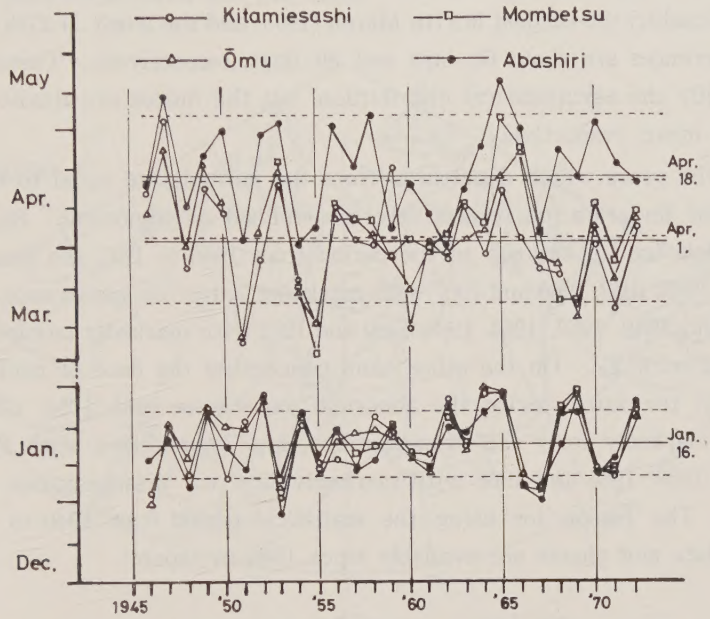

Fig. 2. Inter-annual variations of the dates of pack ice appearance (lower part) and disappearance (upper part) along the Okhotsk coast of Hokkaido. Broken lines indicate standard deviation (σ).

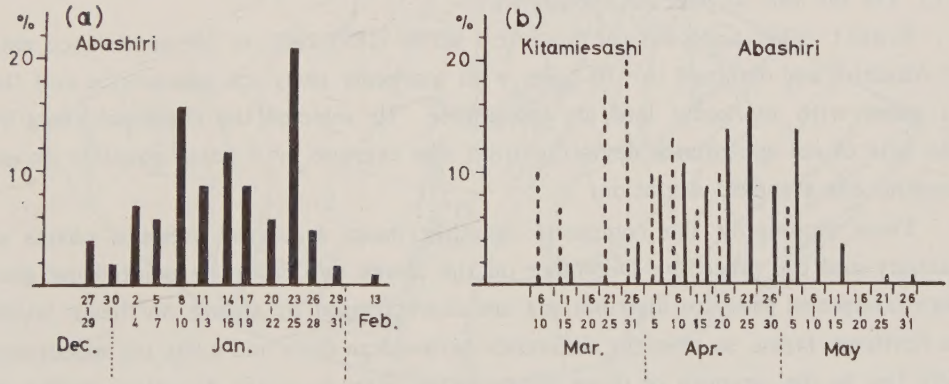

Fig. 3. Histograms of the dates of pack ice appearance and disappearance. (a) appearance at Abashiri, (b) disappearance at Kitamiesashi (broken line) and Abashiri (solid line).

is 27th December (1952) and the latest is 13th Feburary (1903), so the difference is about 50 days. The histogram shows roughly a bimodal distribution, namely, the classes of Jan. 8th~10th and Jan. 23rd~25th. The earliest date of pack ice disappearance at Kitamiesashi is 6th March (1951) and the latest date is 3rd May (1944, 1947), at Abashiri the earliest is 11th March (1903) and the latest is 27th May (1944), so the differences are about 60 days and 80 days, respectively. These histograms show roughly the asymmetrical distribution, but the modes are almost equal to the arithmetic mean, respectively.

Here, the years which departures from the normals are equal to or exceeding the standard deviation (σ), respectively, are defined as abnormal. Regarding the date of pack ice appearance in the period from 1946 to 1972 the abnormal years were 1946, 1948, 1953, 1966 and 1967 with markedly early ice appearance (symbolized with Y_1) and 1949, 1952, 1964, 1965, 1969 and 1972 with markedly late ice appearance (symbolized with Y_2). On the other hand concerning the date of pack ice disappearance in the same period the abnormal years were 1951, 1954, 1955, 1962 and 1969 with markedly early ice disappearance date (symbolized with Y_3) and 1947, 1949, 1953, 1958, 1965 and 1966 with markedly late ice disappearance (symbolized with Y_4). The reason for using the statistical period from 1946 to 1972 is that upper-air data and charts are available since 1946 in Japan.

3. Relationships between the dates of pack ice appearance or disappearance and atmospheric circulation

(1) On the date of pack ice appearance

SCHELL (1964) analysed the historical series (1899–1961) of ice appearance date at Abashiri, and obtained the 10 cases with markedly early ice appearance and the 11 cases with markedly late ice appearance. He selected the abnormal years by the date of ice appearance deviating from the average by a value equal to or exceeding one standard deviation.

From examining the composite monthly mean sea level pressure charts of January and the preceding December on the above two cases, he pointed out that both composite pressure distributions are characterized by strong northerly winds in northern Japan, so that the difference between an early and a late ice appearance date lies in the strength of these winds rather than in their direction insofar as northern Japan is concerned. Further he obtained the moderate relationships between the date of pack ice appearance at Abashiri and the mean monthly January

pressure gradient over the northern Okhotsk Sea, the correlation coefficient $r = -0.48$ and similarly $r = -0.47$ for the preceding December pressure gradient upstream over northeastern Siberia. However, there was not a marked difference in the pressure distribution pattern between the two cases.

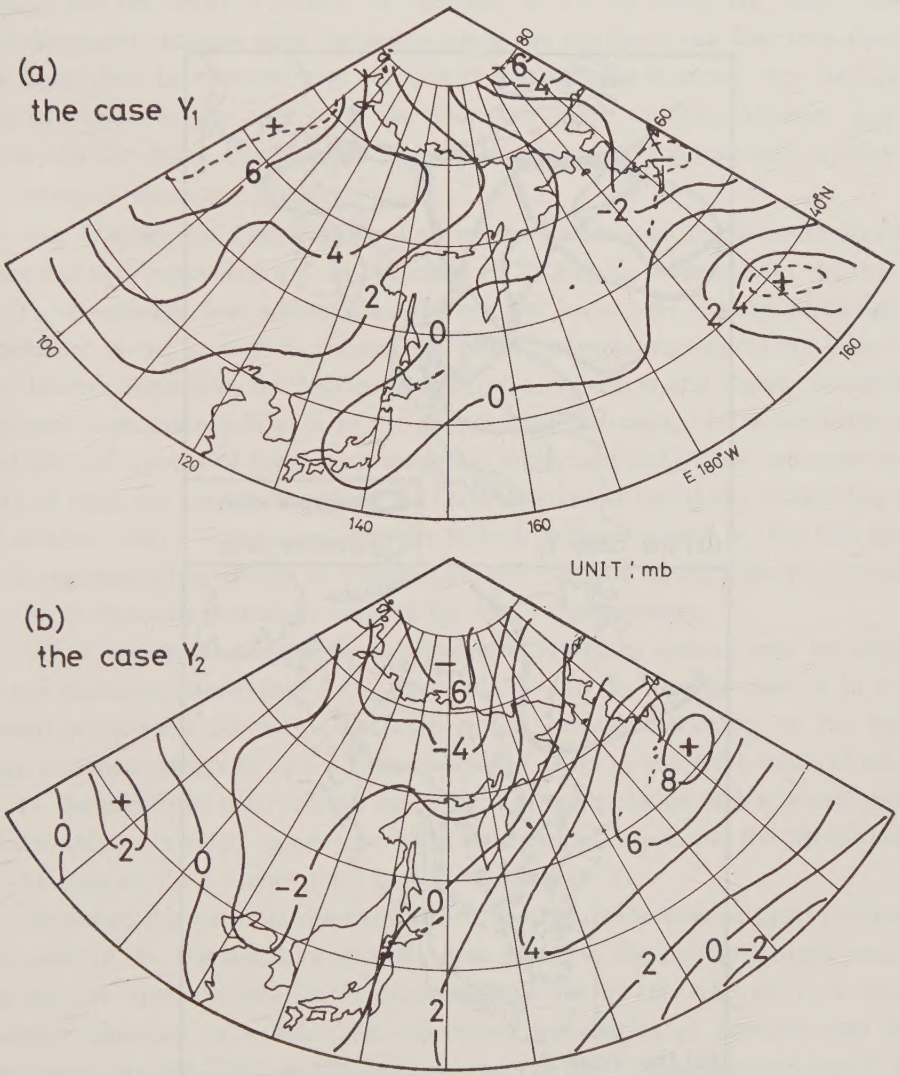

Fig. 4. Composite charts of sea level pressure anomaly in preceding December in the abnormal years with markedly early ice appearance (Y_1) and with markedly late ice appearance (Y_2).

In order to more clarify the differences of character of pressure distribution in abnormal years, the composite charts of sea level pressure anomaly from normal in the above mentioned Y_1 and Y_2 cases were examined by the present author, though their statistical period are differ from SCHELL's. As seen in Fig. 4, there is marked difference between the two anomaly distribution charts for Y_1 and Y_2.

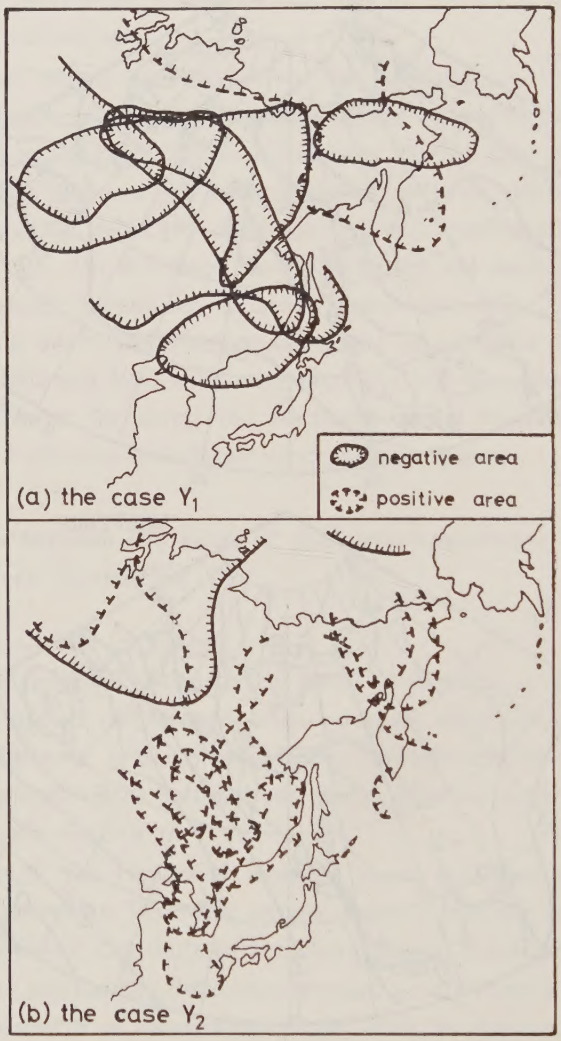

Fig. 5. Distribution of areas where surface air temperature anomalies in preceding December are equal to or exceding 4°C in the cases of Y_1 and Y_2.

In the case of Y_1, the area of above-normal anomaly exists on the continent from Siberia to China, and the area of below-normal anomaly exists in the sea area from the Bering Sea to the Kuriles; in the case of Y_2, in constrast to the case of Y_1, the area of above-normal anomaly exists in the north of the North Pacific, and the area of below-normal anomaly exists in the region from the Arctic Sea to Siberia and the north of China. In the case of Y_1 the Shiberian High develops and developed cyclones pass frequently along the Kuriles to the Aleutians, therefore the N-ly~NW-ly monsoon with outburst of cold air mass is strong over the Okhotsk Sea; conversely in the case of Y_2 the Shiberian High and the Aleutian Low are weak and the North Pacific High shifts northward, so the monsoon is weak and advection of warm air mass occurs.

Fig. 5 shows the distributions of areas where surface air temperature anomalies are equal to or exceeding 4°C in the cases of Y_1 and Y_2, respectively. In the case of Y_1 remarkedly low temperature regions are found over Siberia, Saghalien and Hokkaido; in the case of Y_2 remarkedly warm temperature regions are found over the Taimyr Peninsula, the Maritime Provinces of Siberia and Korea, moreover on the area from eastern Siberia to the Kamchatka Peninsula. It is comprehensible that the differences of these meteorological conditions have close influence on the date of pack ice appearance along the Okhotsk coast of Hokkaido. (CHISHIMA, 1962; AKAGAWA, 1967). The reason why the 500-mb surface is used is that this surface is a representative surface of troposphere and the data of atmospheric circulation on the surface are frequently utilized for long-range forecast.

Fig. 6 shows the composite charts of monthly mean contour and its anomaly in the preceding December in the cases of Y_1 and Y_2. In the case of Y_1 a deep trough with polar vortex on the north of the Okhotsk Sea exists in the eastern edge of Asian continent and a ridge seems to exist in the Ural; while in the case of Y_2 the centre of polar vortex exists in the Arctic region and a trough extends southward and a ridge seems to exist in the Alaskan region, and the 500-mb surface in the case of Y_2 is higher than that in the case of Y_1.

However, the anomaly distributions of the two cases show a great contrast; in the case of Y_1 the negative anomaly area exists in the middle latitude zone and the positive anomaly area in the other regions, but in the case of Y_2 a entirely contrary tendency is found. The coincident frequencies of anomaly sign in the two cases are 100~75% in the large anomaly areas. These features nearly equal to the results that Kato (1969) obtained on the relation between types of zonal index and percentages of sign occurring of 500-mb height anomalies.

These situations are explained meteorologically as follows:—In the case of Y_1, the so-called low index circulation is predominant and meandering flow with meridional circulation is active, so cold air expands over the middle latitude though energies of cold air in the high latitude become weaker; on the other hand, in the case of Y_2 the so-called high index circulation is predominant and zonal flow is

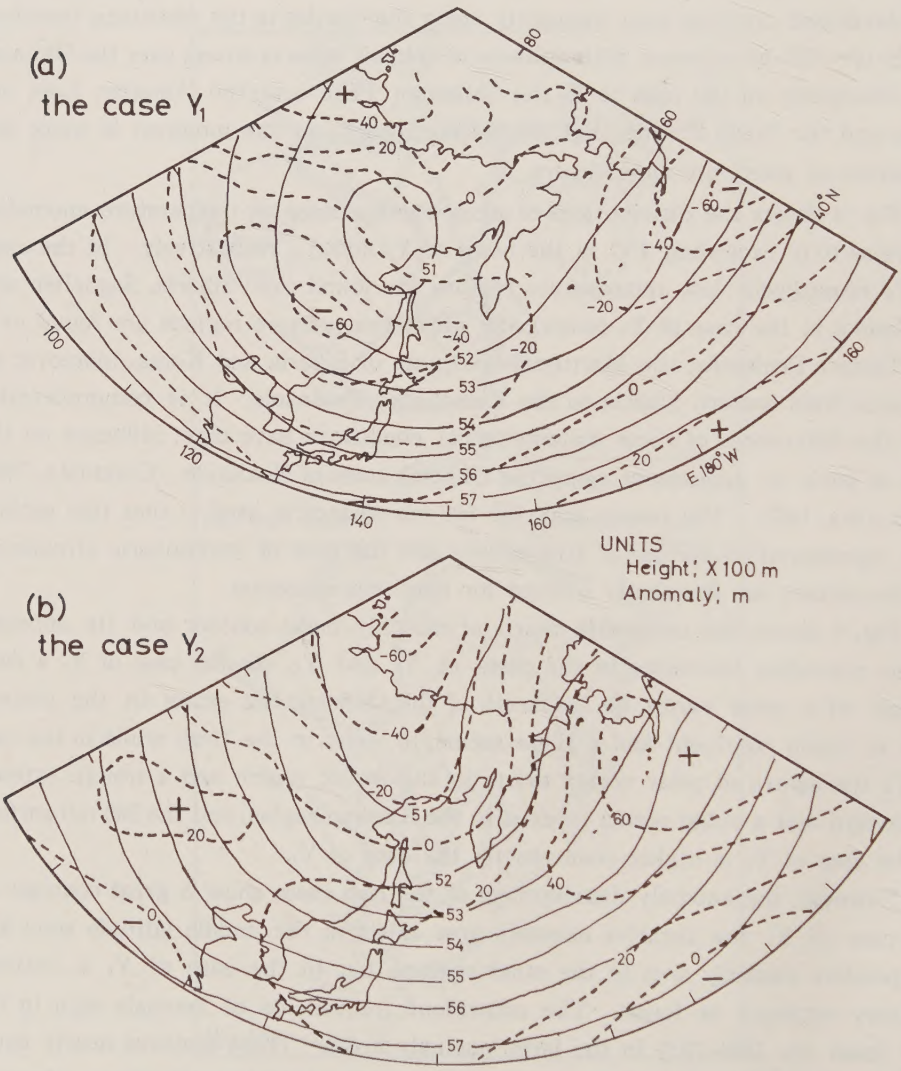

Fig. 6. Composite chart of monthly mean 500-mb height contour (solid line) and its anomaly (broken line) in preceding December in the cases of Y_1 and Y_2.

active, so both energies of cold air in the high latitude and warm air in the middle latitude are strong and outburst of cold air to the Far East is weak. It would be comprehensible that such upper-air conditions are related to the date of pack ice appearance along the Okhotsk coast of Hokkaido.

As for features of the 500-mb atmospheric circulation in the preceding November, in the case of Y_1 the southward shift of polar vortex is vivid and large negative anomaly area exists mainly over Baikal to the Okhotsk Sea and positive anomaly area exists over the Arctic to the Alaskan Bay; but in the case of Y_2 the anomaly sign is the very reverse to that of the case Y_1. These features are generally similar to those in December above mentioned, but the centres of the areas of positive or negative sign in November lie more westward than in December, that is, features of atmospheric circulation which relates to abnormal sea ice conditions appear in November more westward areas than in December.

SCHELL (1964) also indicated in his study as follows: stronger or weaker northerly winds in January are preceded by stronger or weaker, respectively, similar winds in December, leading to a marked relationship also with the December winds upstream and the farther back in time an event is considered, the farther upstream its control will originate, provided the circulation pattern maintains a certain

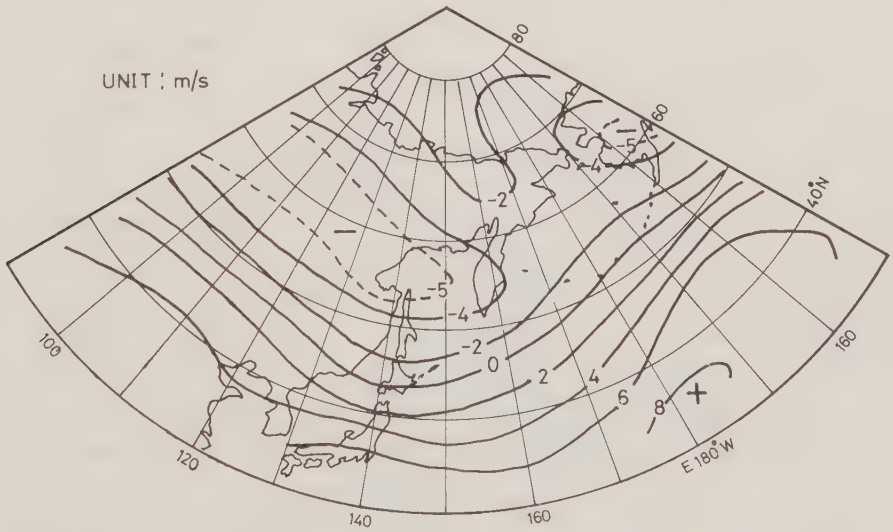

Fig. 7. Difference of the westerly component of wind velocity of geostrophic wind on the 500-mb surface between the cases of Y_1 and Y_2. Positive sign means that the westerly component of wind velocity in case of Y_1 is larger than that in case of Y_2, and negative means its reverse.

continuity. These relationships should be utilized for long-range sea ice forecasting.

Moreover, character of upper-air flow in each case was investigated. Zonal and meridional components of geostrophic wind were calculated respectively from the monthly mean charts of the 500-mb height.

In the case of Y_1 the westerly component is weaker than normal north of about 50°N zone (centred 60°N) and in Siberia changes to the easterly component, but stronger south of that than normal. In the case of Y_2 the westerly component is stronger north of about 45°N and weaker south of that. These characters are seen in Fig. 7 showing the difference of the westerly component between the cases of Y_1 and Y_2.

On the meriditional component, the area near 140°E is a boundary between the northerly component area and the southerly component area in the cases of Y_1 and Y_2, and the difference between the two cases is shown in Fig. 8. Compared with the case of Y_2, the northerly component in the case of Y_1 is stronger over the Taimyr Peninsula, northern part of China, Korea and Japan and weaker on the Maritime Provinces of Siberia, and the southerly component is stronger over the eastern sea of Japan and the Okhotsk Sea and weaker over the Arctic Sea, the Bering Sea and southeast of it. These indicates clearly that in the case of Y_1 meridional circulation

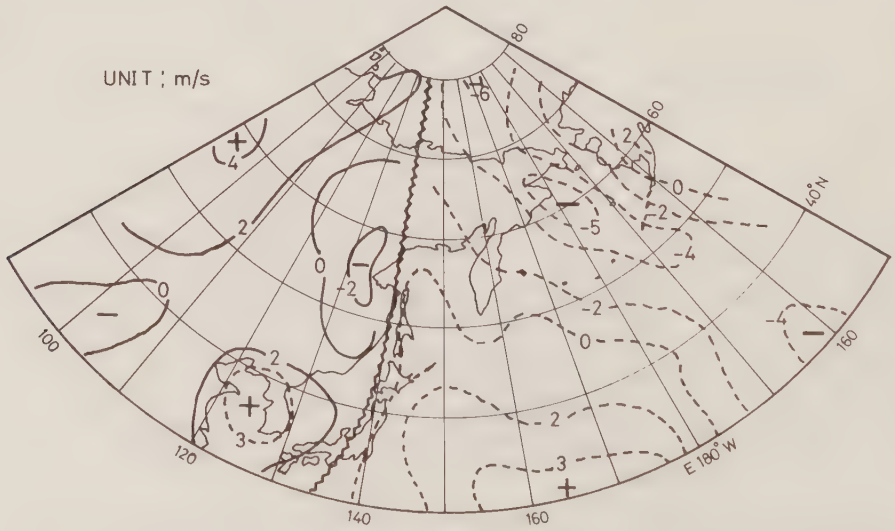

Fig. 8. Difference of the meridional component of wind velocity of geostrophic wind on the 500-mb surface between the case of Y_1 and Y_2. Solid line: northerly component, broken line: southerly component. Positive and negative signs are the same as those in Fig. 7.

is predominant around the southern polar vortex, but in the case of Y_2 zonal flow prevails as mentioned above.

(2) *On the date of pack ice disappearance*

As for the date of pack ice disappearance, features of atmospheric circulation in March were examined in the same way as described in (1). Fig. 9 shows the

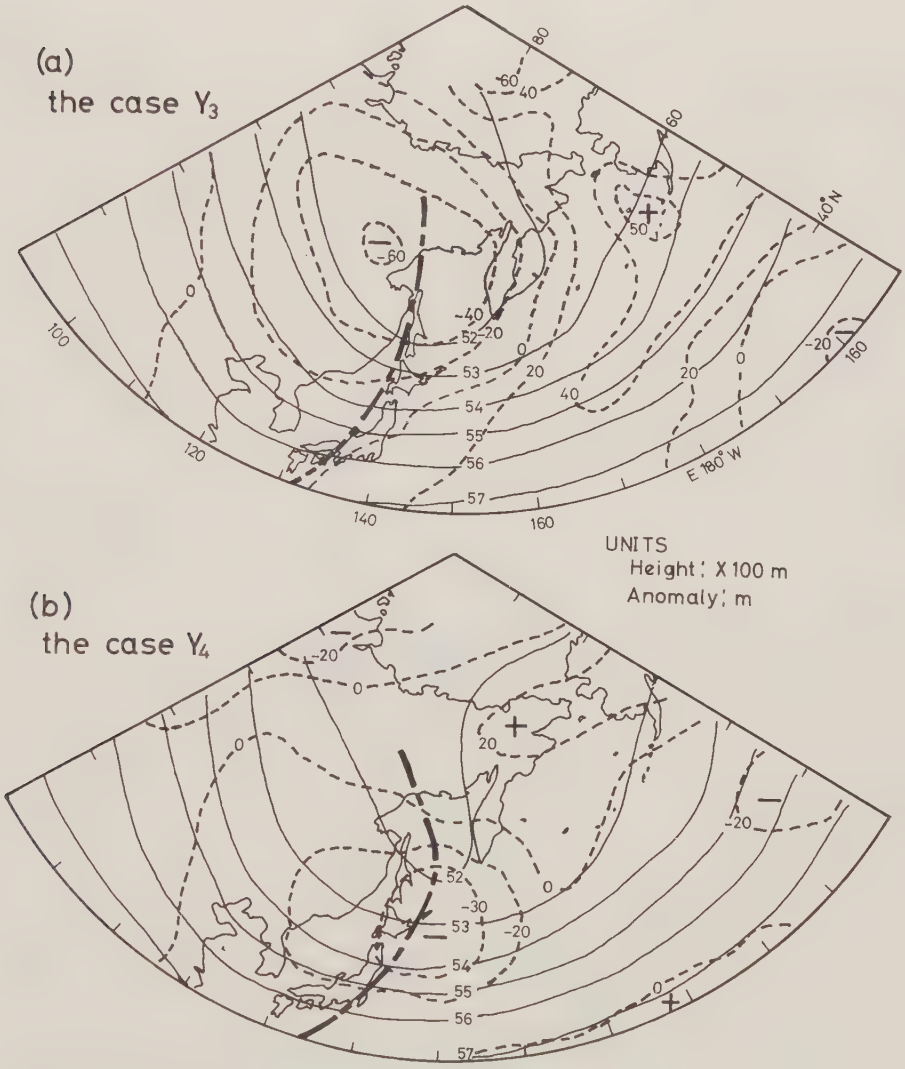

Fig. 9. Composite charts of monthly mean 500-mb height contour (solid line) and its anomaly (broken line) in March in the cases of Y_3 and Y_4.

composite charts of monthly mean 500-mb height contour and its anomaly in March in the case of Y_3 (markedly early ice disappearance) and in the case of Y_4 (markedly late ice disappearance). There is generally no difference between the two cases except for the distribution of contour in Siberia region and the position of trough in the Okhotsk Sea and Hokkaido, but as for the anomaly distribution striking

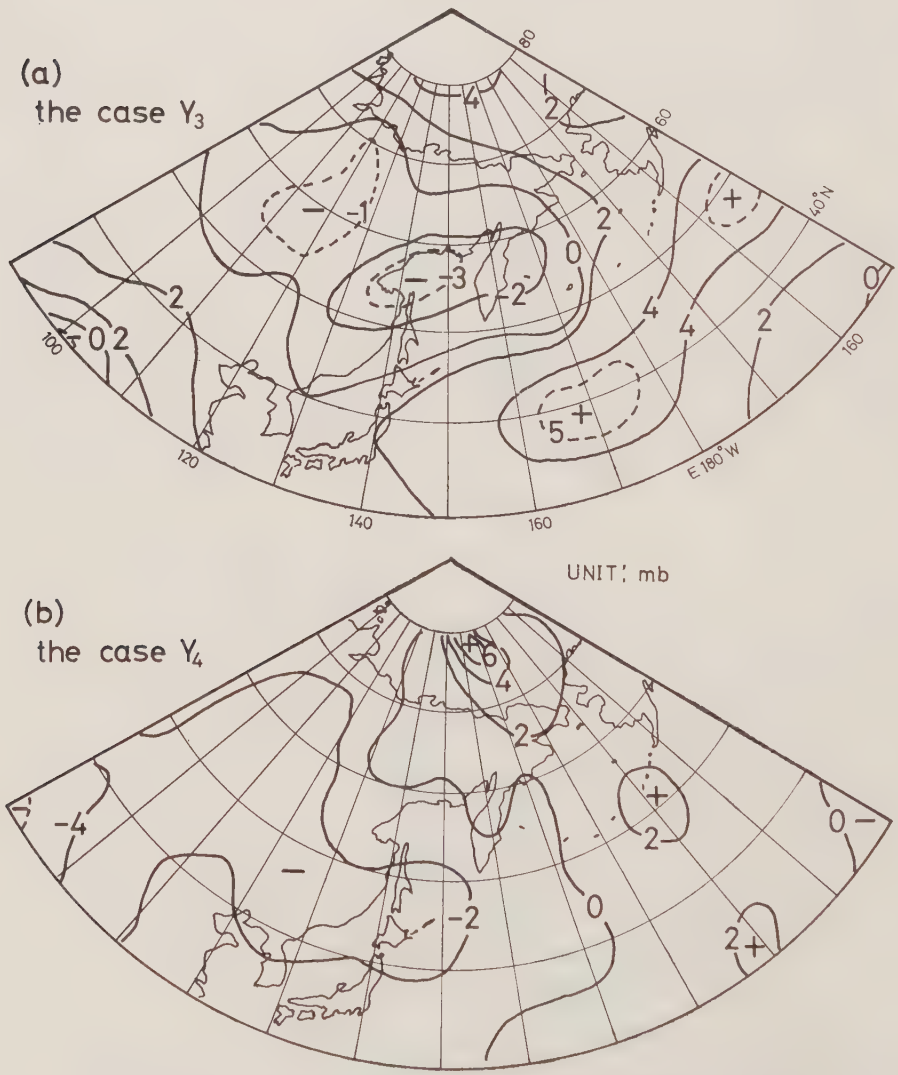

Fig. 10. Composite chart of sea level pressure anomaly in March in the cases of Y_3 and Y_4.

contrasts are seen.

In the case of Y_3 the negative anomaly area exists in the Far East (centred around 57°N, 130°E) and the positive anomaly area exists in the North Pacific, the Bering Sea and the Polar region, accordingly in the southern part of the Okhotsk Sea the so-called south-high and north-low pressure pattern is formed and this situation is regarded as the high index circulation.

In the case of Y_4 the negative anomaly area exists in the middle latitude zone (centred in Hokkaido and The Kuriles) and the positive anomaly area over Alaska, the Bering Sea and eastern Siberia, accordingly in the Okhotsk Sea the so-called north-high pressure pattern is formed and this situation is regarded as the low index circulation. It is noted that these two cases show contrary features in the Okhotsk Sea. The coincident frequencies of anomaly sign in these cases also are above 75% in the large anomaly areas.

Further these situation were discussed in connexion with sea level pressure anomaly in the cases of Y_3 and Y_4. In the case of Y_3 the negative anomaly area exists in the northern part of the Okhotsk Sea and central Siberia, and the positive anomaly area exists widely in the northern part of the North Pacific Ocean. In the case of Y_4 the negative anomaly arer exists widely in the area from Japan to Asian continent and the positive anomaly area extends from the Arctic to the Bering Sea and the North Pacific Ocean. Moreover, character of upper-air flow on the 500-mb surface was examined from geostrophic wind.

On the pattern of the westerly component, there is little difference between the two cases and in both cases area of weak easterly component exists in eastern Siberia. However, inspecting the anomaly from normal, in the case of Y_3 stronger area of the westerly component exists zonally centred around Hokkaido and in the case of Y_4 weaker area extends zonally centered in the Okhotsk Sea. These character is seen in Fig. 11 showing the difference of the westerly component between the cases of Y_3 and Y_4.

As for the meridional component, characters of distribution pattern in the two cases resemble each other on the whole; that is, the region from the Lena River Basin to Saghalien and Japan divides the northerly component area on the west from the southerly component area on the east, and both areas are stronger than normal in the two cases. However, it is noted that in the case of Y_3 the anomalies from normal are larger and the centre of the southerly component area exists more northwards and the dividing boundary between the northerly component area and the southerly component area lies more eastward than situations in the case of Y_4.

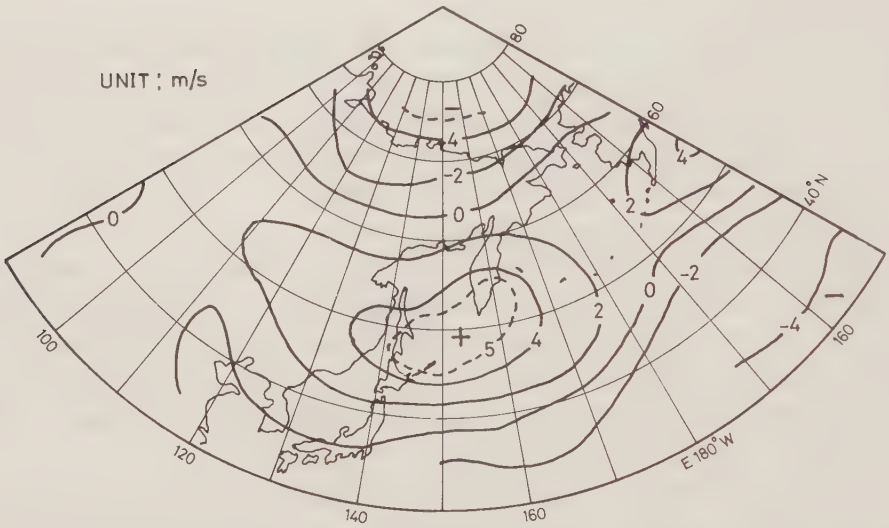

Fig. 11. Difference of the westerly component of wind velocity of geostrophic wind on the 500-mb surface between the cases of Y_3 and Y_4. Positive sign means that the westerly component of wind velocity in case of Y_3 is larger than that in case of Y_4, and negative means its reverse.

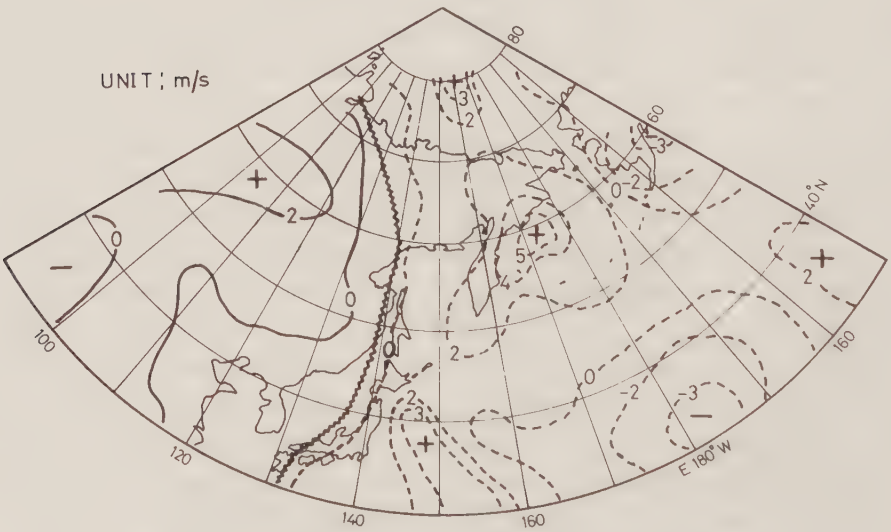

Fig. 12. Difference of the meridional component of geostrophic wind on the 500-mb surface between the cases of Y_3 and Y_4. Solid line: northerly component, broken line: southerly component. Positive and negative signs are the same as those in Fig. 11.

These characters are seen in Fig. 12 showing the difference of the meridional component between the cases of Y_3 and Y_4.

In synthesizing these situations, following meteorological features can be suggested. In the case Y_3, that is, in the years with markedly early ice disappearance, upper trough is to the west of the Okhotsk Sea and negative anomaly area of pressure exists in the northern part of the Okhotsk Sea and ridge in the North Pacific Ocean develops. These involve tendencies of passing of lows in the north of Hokkaido and developing or northing of the North Pacific High. Accordingly, along the Okhotsk coast of Hokkaido southerly or westerly winds prevail and the winds make the pack ice move away from the coast.

On the other hand, in the case of Y_4, that is, in the years with markedly late ice disappearance, upper trough crosses the central part of the Okhotsk Sea and negative anomaly area of pressure exists in Hokkaido and ridge from Alaska to eastern Siberia is also noted. These involve tendency of passing of low in Hokkaido and its neighbourhood and suggest the so-called Blocking action. Accordingly, along the Okhotsk coast of Hokkaido north-easterly or north-westerly winds which keep the pack ice until late along the coast blow very frequently.

It can be concluded that whether pack ice disappearance along the coast of Hokkaido is early or late is mainly influenced by wind system in the Okhotsk Sea related with position of trough and track of low.

As for the influence of air temperature on disappearance of pack ice, Fig. 13 shows the distributions of areas where surface air temperature anomalies are equal to or exceeding 2°C in the cases of Y_3 and Y_4. The reason why the limit of 4°C in the same manner as in the cases of Y_1 and Y_2 is not adopted is that in the cases of Y_3 and Y_4 such large anomaly as above 4°C is scarce. Here, it is noticed that systematic features in the anomaly distribution are not found differing from Fig. 5. SCHELL (1964) obtained 12 cases with markedly early ice disappearance date and 12 cases with markedly late ice disappearance date from analizing the historical series (1899–1961) of ice disappearance date at Abashiri.

From examining the composite monthly mean sea level pressure charts of April in the above two cases, he also pointed out as follows:—The direction of the winds to the north of Japan in the average case with markedly late ice disappearance date is northerly, while the direction of the winds over Hokkaido in the average case with markedly early ice disappearance date is, on the whole, from west-southwest; similarly the direction of the geostrophic winds over Japan in the preceding March is from the northwest for the group of cases with markedly

early ice disappearance date, but is from the north-northwest for the group of cases with markedly late ice disappearance date.

Moreover, he indicated a moderate relationship between the ice disappearance date at Abashiri and the April monthly mean pressure gradient centred around 45°N and 145°E, but little, if any, relationship with the gradient to the north in

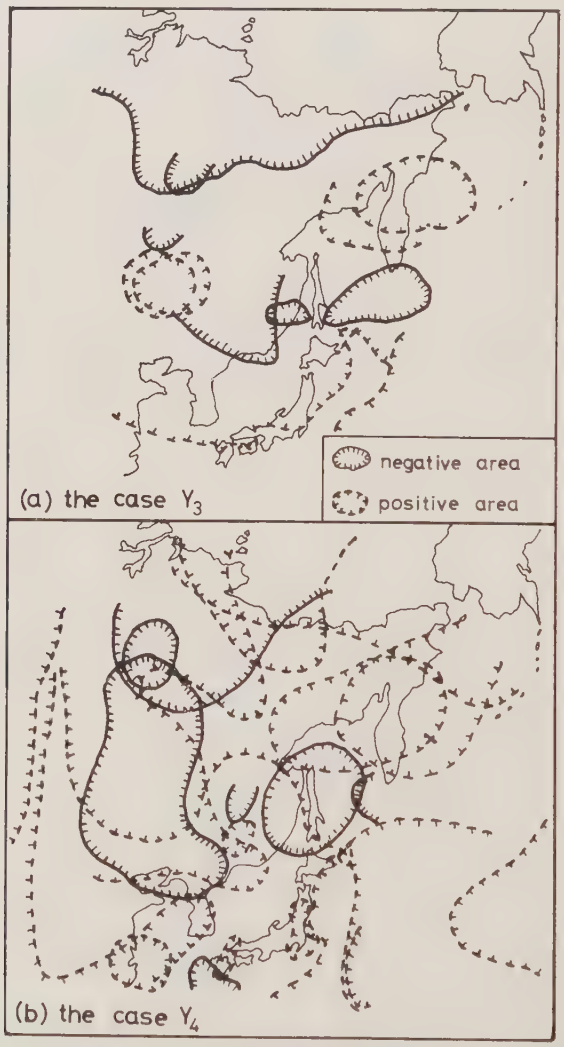

Fig. 13. Distribution of areas where surface air temperature anomalies in March are equal to or exceeding 2°C in the cases of Y_3 and Y_4.

March, presumably because of the discontinuous change in the general circulation during the spring in that general area.

Some researches of relations between atmospheric pressure pattern and the date of pack ice disappearance along the Okhotsk coast of Hokkaido were made in connexion with long-range sea ice forecasting in Japan. SEGAWA (1960) created an index ΔI for change of ice amount, that is, $\Delta I=(P_{Sapporo}-P_{Nemuro})-(P_{Urakawa}-P_{Haboro})$ in March, $P=$ sea level pressure, and obtained the correlations with sea ice conditions at Abashiri; $r=+0.77$ for pack ice amount in March, $r=+0.39$ for pack ice amount in April, $r=+0.55$ for the date of pack ice disappearance and $r=+0.68$ for the date of "Umiake" (ice amount in sight from coast $<5/10$. That means the beginning of navigation or fishery), respectively. HATA (1966) obtained a marked relation the pressure gradient (55°~30°N along 140°E) in February and the date of "Umiake" at Mombetsu; however, the correlation has declined in recent years.

4. Summary and discussion

In this paper the character of atmospheric circulation in the years of abnormal sea ice conditions along the Okhotsk coast of Hokkaido was studied. The strength of monsoon wind system in December in the Far East has great influence on the date of pack ice appearance and the role of cold air mass in Siberia Continent is also important as seen in the distribution of air temperature anomaly. On the effect of temperature, SCHELL (1964) also suggested that the temperature of northern Hokkaido and, perhaps, even more so those at stations to the north of Japan, similarly reflect an important control of the ice appearance dates in Hokkaido.

As for atmospheric circulation type, the low index type, namely meridional circulation type, corresponds to the case with markedly early pack ice appearance and the high index type, namely zonal circulation type, corresponds to the case with markedly late pack ice appearance. Features of the 500-mb atmospheric circulation in the preceding November are generally similar to those in December and these relationships should be available for long-range sea ice forecasting. On the other hand, the date of pack ice disappearance is rather affected by wind direction due to atmospheric pressure pattern as north-high or south-high, position of upper trough and track of low.

Here, it is questionable that any systematic features in the air temperature anomaly distribution for pack ice disappearance do not exist. It is permissible to consider as follows:—The period of pack ice coming, that is, from December to

January, is a simple stage called winter in the light of the seasonal changes of a year, and the strength of the monsoon plays the leading role for pack ice appearance and air temperature is subordinate to the behaviour of the monsoon. However, the period of pack ice leaving, from March to April, is the changing stage from winter to spring, so the pressure pattern in the period is unstable. Moreover, in the period of pack ice leaving closeness of ice area is generally small and movement of pack ice is rapid, so wind direction in the period has an important effect on pack ice disappearance.

On the other hand, the weasterly wind which makes pack ice move away from the Okhotsk coast of Hokkaido does not necessarily accompany warm air which helps to melt pack ice and the easterly wind which keeps pack ice until late along the coast does not always accompany cold air which delays thawing, or rather are there the contrary cases respectively. These would be the reason why any systematic features in the temperature anomaly distribution for pack ice disappearance are not found.

CHISHIMA (1962) obtained the simultaneous correlations between the air temperature and the pack ice amount at Abashiri, $r=-0.66$ for January, $r=-0.58$ for February, $r=-0.30$ for March and $r=-0.61$ for April, and also on the one-month lag-correlations between the monthly pack ice amount, $r=+0.50$ for January-February, $r=+0.08$ for February-March, $r=0.82$ for March-April. It is noticeale that March is a unique and special month. The above-mentioned facts are also associated with the hardness of long-range sea ice forecasting on the date of pack ice disappearance (AKAGAWA, 1967).

There are following studies of the relations between atmospheric circulation and the ice conditions in the East Greenland Current or in Iceland. STRUBING (1967) indicated that the amount of ice carried by the East Greenland Current is preceded by a wind-produced influx of ice from the Arctic Ocean largely influenced by the atmospheric circulation over the Arctic Ocean and the reflections might be worth considering in a long-term forecast of the ice mass. BERGTHORSSON (1970) indicated that considering the ocean currents north of Iceland the air temperature of the island of Jan Mayen is thought to be of prognostic value for the ice conditions in Iceland approximately half a year in advance, and formulated the correlation adding the effect of easterly wind component north of Northwest-Iceland. RODEWALD (1971) also showed that the drift of the arctic pack ice into the Iceland sea area is related to the atmospheric circulation over the Arctic Ocean.

On the one hand, Sanderson (1971) described as follows:—Attempt to relate the

movement of the ice edge over the Greenland Sea with the mean wind, as has been done successfuly elsewhere, at least over periods of a few days, have failed to account satisfactorily for the abnormal rates of advance that have sometimes occurred, even when the effects of current, new freezing, etc. have been taken into account. It is suggested that this is mainly because the prevailing wind direction over the area is such that it has only a small component at right angles to the ice edge. If the ice edge movement is related instead to the mean wind anomaly, i.e. to the departure of the mean wind from its long-term value, then abnormal rates of advance are more satisfactorily explained, being associated with substantial wind anomalies from the north-west or west quadrants. It is hoped that monthly forecasts of the sea-ice conditions over the Greenland Sea may be made, as forecast charts of the mean monthly surface-pressure become available. These studies have the same idea as the present author. After this, it is necessary for long-range sea ice forecasting to quantify the correlations obtained from this study.

Acknowledgement

The author wishes to express his deep thanks to Mr. S. Tashiro of the Hakodate Marine Observatory and Dr. WATANABE of the Kyoto Gakuen University for their valuable advices. This work was partially supported by the Japan Society for Promotion of Science as a part of the United States-Japan Cooperative Science Program (4R-005).

References

AKAGAWA, M. (1967): Practical method for long range sea ice forecasting. *Technical Report of JMA.*, **No. 59**, 85–118.

ARMSTRONG, T. (1955): Soviet workes on sea-ice forecasting. *Polar Record*, **7**, 302–311.

BERGTHÓRSSON, P. (1970): Forecasting drift ice at Iceland by means of Jan Mayen air temperature. *Jökull*, **19**, 44–52.

CHISHIMA, S. (1962): On the sea ice at Abashiri. *J. Met. Res.*, **14**, 639–673.

HATA, R. (1966): Forecasts for the appearance time and the thawing time of drift-ice. *Technical Report of JMA.*, **No. 49**, 68–71.

KATO, H. (1969): Characteristics of monthly mean zonal index and 500 mb height anomaly field. *J. Met. Res.*, **21**, 377–386.

KUSUNOKI, K. (1955): Recent advances in the study of sea ice. *Low Temperature Science, Ser. A.*, **14**, 155–184.

RODEWALD, M. (1971): Der Arktische Umschwung. *Umschau*, **6**, 205–207.

SANDERSON, R.M. (1971): Ice-edge movement in the Greenland Sea. *Marine Observer*, **41**, 173–183.

SCHELL, I.I. (1964): Interrelation of the ice off northern Japan and the weather. *J. Met. Soc.*

Japan, Ser. II, **42**, 174–185.

SEGAWA, T. (1960): Relations between winds and pack ice amount and final date of pack ice disappearance at Abashiri. *Seppyō* (*Journal of the Japanese Society of Snow and Ice*), **22**, 82–84.

STRÜBING, K. (1967): Über Zusammenhänge zwischen der Eisführung des Ostgrönlandstroms und der atmosphärischen Zirkulation über dem Nordpolarmeer. *Deutsche Hydrographische Zeitschrift*, **20**, 257–265.

WIESE, W. (1924): Polareis und atmosphärische Schwankungen. *Geogr. Ann.*, **6**. [See Albert DEFANT (1961): Physical Oceanography. Pergamon Press, Oxford, Chapter VIII Sea Ice]

北海道オホーツク海沿岸の異常海氷年における大気循環の特徴

赤　川　正　臣

（函館海洋気象台）

北海道オホーツク海沿岸の海氷観測資料（1946–1972）から流氷初・終日の平年偏差が標準偏差以上の年をそれぞれについての異常海氷年と定義した。初日に対しては前年12月，終日に対しては3月の平均的な極東域の大気循環の特徴を地上気圧・気温，500 mb 面環流の平年偏差の観点から検討してみた。

流氷初日のはやい，おそいは大陸高気圧の発達，アリューシャン低気圧・北太平洋高気圧の動向に左右される。すなわち季節風の強弱が支配因子で，気温偏差分布もきわめて対称的である。環流型は初日のはやい年が南北循環型で，おそい年は東西流型である。11月にさかのぼれば 500 mb 面に12月の特徴がもっと西に偏した分布で見られる。

流氷終日のはやい・おそいは，上層の谷の位置や低気圧の経路に左右される。オホーツク海では終日のはやい年は南高型気圧配置，おそい年は北高型である。

したがって，流氷の沿岸での停滞，退去は到来期と異なって風速よりも風向に支配されている。気温偏差分布も12月のように整然としていない。これは流氷到来期，退去期における季節変化過程の安定性の相違に依っている。

これらの特徴は長期海氷予報に利用されるが，今後はさらにその量的関係の見積りが望まれる。

The Oceanographical Magazine
Vol. 24, No. 2, pp. 101 to 105, March 1973

A Note on the Palaeogeographic Location of Trenches

Nozomu DEN and Masashi YASUI

Meteorological College, Kashiwa, 277 Japan

(Received 9 December 1972)

Abstract: Locations of the presnt trenches and the Alpine-Himalaya orogenic belt are marked on the map of the continents as of the end of the Palaeozoic era. It is then found that the circum-Pacific trench system marginates the universal landmass of Pangaea as the circum-Pangaean trench system. This palaeogeographic distribution suggests that the present trenches might still be influenced by the tectonic processes occurred in the marginal region of Pangaea.

The resent trenches develop along the continental margins or island arcs and border the Pacific Ocean with the exception of a few trenches, such as the Java Trench. The trench is believed to be the site where the related oceanic lithosphere is being subducted into the mantle. From this point of view the trench is a part of the presently active tectonic element. However, to examine the relationship between the trench and the old tectonic process in the geologic history is of interest and importance in order to elucidate the origin of the trench.

Reconstruction of the continents into Gondwanaland or Pangaea has been presented in the different ways by many authors (e.g., DIETZ and HOLDEN, 1970). In the present discussion at least major geographical features of Pangaea is required although the details are not always necessary. Figure 2 in the paper by DIETZ and HOLDEN (ibid) is cited as a world map as of the end of the Permian period (Fig. 1). Then the location of the recent trenches is put on their reconstruction map with bold lines keeping the positions of the trenches relative to the adjacent continents to be the same as the present ones. To make the situation much understandable, the present arrangement of trenches is also shown in Fig. 2. All of the trenches excluding the Puerto Rico and South Sandwich Trench are recognized along the margins of the single supercontinent of Pangaea and never appear either inside nor far away off Pangaea. Moreover even the South Sandwich Trench can also be situated close to the southwestern margin of it, if the map of the Gondwanaland reconstructed by HURLEY and RAND (1969) is reffered to. However, the Puerto Rico Trench (MOLNAR and SYKES, 1969) and South Sandwich Trench are

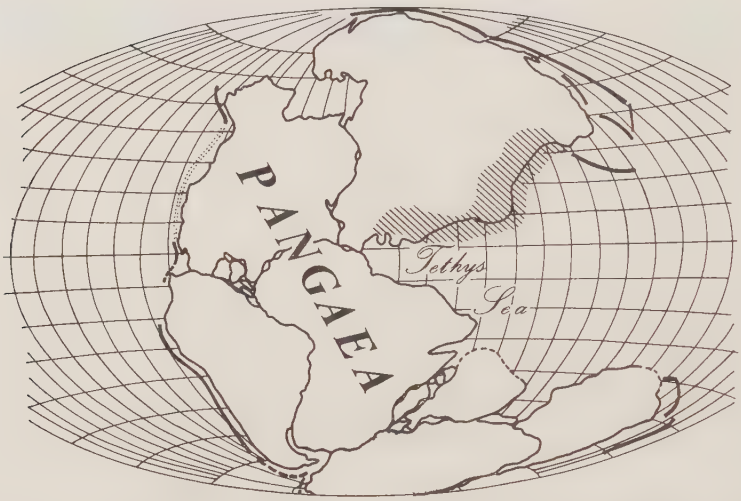

Fig. 1. Trenches and Alpine-Himalayan orogenic belt drawn on the map of Pangaea (DIETZ and HOLDEN, 1970) as of the end of Permian. Bold lines; trenches. Broken lines; buried trenches. Double dotted lines; trenches supposedly disappeared during Late Cretaceous. Hatched belt; Alpine-Himalayan orogenic belt.

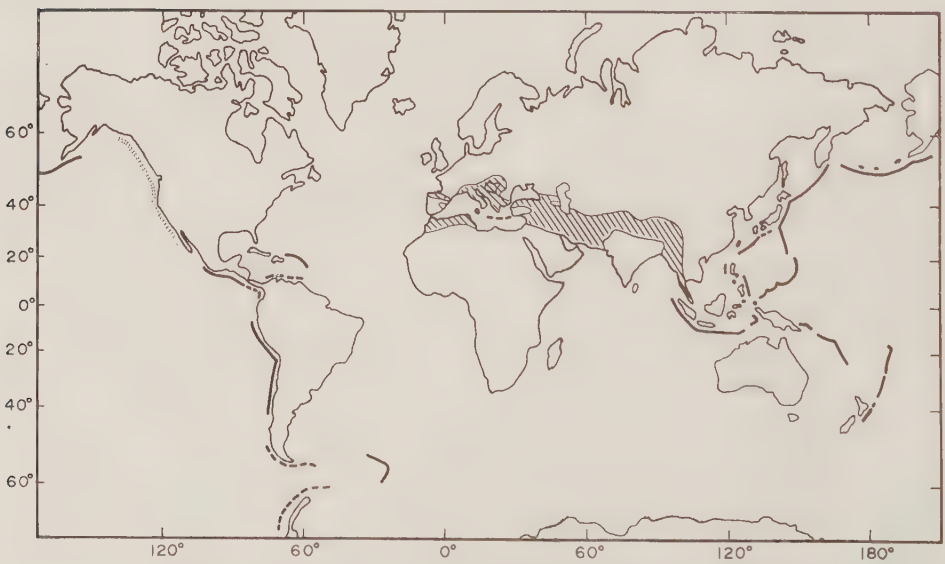

Fig. 2. Present location of trenches and Alpine-Himalayan orogenic belt. See Fig. 1 for the explanatory notes.

considered here to be of somewhat different origin and of different characters from the other trenches, because they are intercontinental, i.e., located between the North American and South American Continent and between the South American and Antarctic Continent respectively.

Some of the recent trenches may have migrated and changed their positions relative to the adjacent continents as suggested by KARIG (1972); e.g. the Tonga-Kermadec-Hikurangi trench system might once border the eastern margin of the Australian Continent. Such displacements of trenches are not considered to be so large that the major features shown in Fig. 1 have been greatly changed.

Several trench-like or trough-like stractures filled with sediments have been observed by means of seismic profiling surveys. Some of them should be regarded as a kind of trenches which are active at the moment or were active in the geological past. According to the discussion of HAYES and EWING (1970), buried trenches are revealed in the places west of the Strait of Juan de Fuca, in the Gulf of Panama, on both sides of the Drake Passage. Outside the Pacific, filled trenches are also located along the southern margin of the Caribbean Sea (EWING et al., 1970) and in the Mediterranean Sea (RYAN et al., 1970). Almost all of them are also along the margins of Pangaea. The location of them are marked by dashed lines on Figs. 1 and 2. Besides these, a sedimentary trough which seems to have been formed by the Palaeozoic tectonic process associated with the sea-floor spreading in the Proto-Atlantic is reported (DRAKE and KOSMINSKAYA, 1969). This trough is disregarded from the present discussion because of its age.

On the southeastern coast of the Laurasian part of Pangaea, the Alpine-Himalayan orogenic belt can be entered as shown in Figs. 1 and 2 with hatched band. After LE PICHON (1968), a large-scale crustal shortening occurred in this zone as the Indian block moved northwards toward the Asian Continent. It is very plausible that a trench system or systems existed along the margins of Laurasia or/and Gondwanaland.

Now a break in this coronary trench system around Pangaea is in the coastal area west of the North America. PITMAN and HAYES (1968) proposed a hypothesis that a trench had bordered the western margin of the North America during Late Cretaceous to Early Pliocene in order to explain the present pattern in magnetic anomalies in the Gulf of Alaska. HAMILTON (1969) and ERNST (1970) attempted to explain the geologic evolution of California region in the terms of the plate tectonics and hypothesized that a trench existed along the western margin of the North American Continent. The location of them is shown with double dotted

lines in the figures.

Thus the margins of the universal continent of Pangaea are fringed by the present active trenches, the buried trenches, the trenches supposedly disappeared during Late Cretaceous, and the Mesozoic to Cenozoic orogenic belts where trenches seems to have existed. Thus the so-called circum-Pacific trench system seems to be first originated as the circum-Pangaean trench system. Though the present trench itself is very likely one of the young tectonic elements, the palaeogeographic location shown in Fig. 1 suggests that the origination of the recent trench systems was correlated with the old tectonic conditions and that the new trench is hardly originated in the ocean which opened posterior to the Mesozoic era. This means that the differences of thermal conditions in the upper mantle between Pangaea and the surrounding ocean in Late Palaeozoic may have influenced upon the origination of the trench systems along the margins of Pangaea and may be giving effects on the global tectonic movements still at present. These conditions should be taken into consideration in the investigation of the breakup of Pangaea.

Acknowledgement

The authors are grateful to Prof. Seiya UYEDA for his critical reading and comments.

References

DIETZ, R.S. and J.C. HOLDEN (1970): Reconstruction of Pangaea: Breakup and dispersion of continents, Permian to present. *J. Geophys. Res.*, **75**, 4939–4956.

DRAKE, C.L. and I.P. KOSMINSKAYA (1969): The transition from continent to oceanic crust. *Tectonophysics*, **7**, 363–384.

ERNST, W.G. (1970): Tectonic contact between the Franciscan mélange and the Great Valley sequence—crustal expression of a Late Mesozoic Benioff zone. *J. Geophys. Res.*, **75**, 886–901.

EWING, J., M. EWING, T. AITKEN, and W.J. LUDWIG (1968): North Pacific sediment layers measured by seismic profiling. In *the Crust and Upper Mantle of the Pacific Area*, Geophys. Monograph 12, Amer. Geophys. Un., Washington, D.C., 147–173.

EWING, J.I., N.T. EDGAR and J.W. ANTOINE (1970): Structure of the Gulf of Mexico and Caribean Sea. In *the Sea*, **Vol. 4, Part 2**, A.E. Maxwell, Ed., Wiley-Interscience, New York, pp. 321–358.

HAMILTON, W. (1969): Mesozoic California and the underflow of Pacific mantle. *Geol. Soc. Amer., Bull.*, **80**, 2409–2430.

HAYES, D.E. and M. EWING (1970): Pacific boundary structure. In *the Sea*, **Vol. 4, Part 2**, A.E. MAXWELL, Ed., Wiley-Interscience, New York, pp. 29–72.

HURLEY, P.M. and J.R. RAND (1969): Pre-drift continental nuclei. *Science*, **164**, 1229–2142.

KARIG, D.E. (1972): Remnant arcs. *Geol. Soc. Amer., Bull.*, **83**, 1057–1068.

LE PICHON, X. (1968): Sea-floor spreading and continental drift. *J. Geophys. Res.*, **73**, 3661–3697.

MOLNAR, P. and L.R. SYKES (1969): Tectonics of the Caribbean and Middle America regions from focal mechanisms and seismicity. *Geol. Soc. Amer., Bull.*, **80**, 1639–1684.

PITMAN, W.C., III and D.E. HAYES (1968): Sea-floor spreading in the Gulf of Alaska. *J. Geophys. Res.*, **73**, 6571–6580.

RYAN, W.B.F., D.J. STANLEY, J.B. HERSEY, D.A. FAHLQUIST and T.D. ALLAN (1970): The tectonics and geology of the Mediterranean Sea. In *the Sea*, **Vol. 4, Part 2**, A.E. MAXWELL, Wiley-Interscience, New York, pp. 387–492.

海溝の古地理学的位置について

田　　望，安井　正

気象大学校

要　　旨

堆積物で埋りかけているものをも含めた現在の海溝とアルプス・ヒマラヤ造山帯とを，関連大陸との相対位置をそのままに保って，古生代末のパンゲア大陸復元図に記入してるみと，その大陸周辺を縁どり環パンゲア海溝系ともいうべきものを形成する。このことから，海溝そのものは比較的新しい構造単元であるかも知れぬが，現海溝系の生成や存続が古生代の造構過程の影響を受けているに違いないことがうかがわれる。

The Oceanographical Magazine
Vol. 24, No. 2, pp. 107 to 158, March 1973

Geomagnetic Anomalies and Tectonics around the Japanese Islands

Nobuhiro ISEZAKI

Meteorological College, Kashiwa, 277 Japan

(Received 9 December 1972)

Abstract: All the available data on the total intensity of the geomagnetic field in the sea area around Japan are recompiled by using GSFC (12/66) as a reference field. The GSFC (12/66) field well represents the actual field of the area for 1965, but its secular change terms are incomplete. From the observed data in the area, $-23\,\gamma$/yr was chosen as the true secular change correction around Japan.

In the northwestern Pacific off the coast of Japan, clear magnetic anomaly lineations are present, whose peak to bottom amplitudes are 500 to 1,000 γ and wavelengths are 50 to 80 kms. The magnetic anomaly profiles can not be matched with any portion of synthetic profiles based on the present reversal time scale of the polarity of the geomagnetic field. The shapes of magnetic anomalies suggest that the latitude of formation of the sea-floor of the area could be $0°-10°$S. This is a strong support for the 30° nortward drift of the northwestern Pacific seamounts proposed from their palaeomagnetic study. By changing the spreading direction and rate, the magnetic anomaly profiles in the area give a good match with those in the southern adjacent area where the strike of lineations is perpendicular to that in the north. If the magnetic anomalies were caused by the reversals with increased frequency in the late Jurassic, a magnetic bight in this area may be proposed. More thorough magnetic survey data are highly desirable to solve tectonic enigma of the northwestern Pacific Ocean.

In the Japan Sea, elongated magnetic anomalies parallel with the Japan Arc are present. Their peak to bottom amplitude are generally less than 200 gammas and wavelengths range up to 40 kms. All anomalies in the Japan Sea are shifted by -100 gammas. This may be the case for other nearby marginal seas also, i.e. the Okhotsk Sea, the Yellow Sea and the East China Sea. These magnetic characteristics imply that the tectonics of the marginal seas may be quite different from that of typical oceans.

The direct interpretation of magnetic anomalies suggests that magnetic anomalies in the Japan Sea are generated by more or less homogeneous magnetizations while those in the northwestern Pacific by sudden changes in directions of the magnetization and also snggests that the positive or negative magnetic anomalies do not always correspond to the normal or reverse polarity of magnetizations in the source body. The reversal time scale so far determined from magnetic anomalies of the seas by simple models may be improved by this method.

1. Introduction

After the detailed magnetic surveys off the west coast of the United States

conducted by the Scripps Institution of Oceanography, in conjuction with the U.S. Coast and Geodetic Survey magnetic-bathymetric survey project, (MASON, 1958; MASON and RAFF, 1961; VACQUIER et al., 1961; RAFF and MASON, 1961) demonstrated the now famous magnetic anomaly lineations trending north-south with the great and the minor offsets, a great number of magnetic surveys have been carried out to attest the hypothesis of sea-floor spreading (DIETZ, 1961; HESS, 1962; VINE and MATTHEWS, 1963). These surveys revealed many examples of magnetic anomaly lineations disposed symmetrically along either side of the crests of the mid-oceanic ridges over the world (VINE, 1966; PITMAN et al., 1968; DICKSON et al., 1968; LE PICHON and HEIRTZLER, 1968; HEIRTZLER et al., 1968).

Within a central axial zone of a ridge, good correlation was established between magnetic anomaly profiles and dated earth's magnetic-polarity reversals, found both on land and in deep-sea cores (COX et al., 1964; OPDYKE et al., 1966; VINE, 1966). This success allowed, through adopting certain assumptions about the spreading rates, extrapolated dating of the floor of world's major ocean basins as far back as to some 80 m.y.b.p. (HEIRTZLER et al., 1968).

The offsets of magnetic anomaly lineations introduced the concept of a new class of faults, named transform faults, in which the displacement suddenly stops or changes its form and direction in a manner that is not true in transcurrent faults (WILSON, 1965).

MORGAN (1968) and LE PICHON (1968) proposed that the earth's surface is separated into several rigid blocks (plates) and explained the tectonics over the world in terms of the interaction between these blocks. Relative motions of these blocks were shown to be expressed by rigid rotations around the axis determined from the directions of fracture zones, i.e., the transform faults between blocks and and by the width distributions of magnetic anomaly lineations.

Thus, magnetic anomalies and their lineations have come to play a highly significant role in marine geophysics, but it appears that there are as many definitions of magnetic anomaly as magnetic analysts. The World Magnetic Survey has been carried out all over the world by the International Associations of Geomagnetism and Aeronomy. Analytic expression of this field by spherical harmonic expansions have been made by several authors (e.g. CAIN et al., 1965; CAIN et al., 1967). Compromise coefficients of spherical harmonics terms of four models were adopted as an International Geomagnetic Reference Field (IGRF) (1968). Although the quality of its coefficients of secular change terms is still quite unsatisfactory, magnetic anomalies obtained by removing IGRF, corrected for secular changes, from

the observed magnetic data can represent the characteristics of the sea in a region smaller than the wave length of variations expressed by higher terms of IGRF, which is a few thousand kilometers.

In Japan the first magnetic survey at sea around Japan was carried out in 1961 in the Pacific off Sanriku (UYEDA et al., 1962). Since then magnetic surveys in the seas around Japan have been carried out by many individuals and groups (e.g., UYEDA et al., 1967; YASUI et al., 1967; YASUI et al., 1967). Analysis of these magnetic data (YASUI et al., 1967; UYEDA and VACQUIER, 1968; ISEZAKI et al., 1969, 1971) established the following facts: There are strong magnetic lineations trending NE-SW off northeast Japan. The lineations are subparallel to the Kuril arc and appear to extend northeastwards almost to the Emperor seamounts. These lineations are, however, difficult to correlate with those found so far in other parts of world oceans. It may be inferred that they are older than those dated so far. In comparison with the typical magnetic anomaly lineations in the Pacific basin proper, the amplitude of magnetic anomalies in the Japan Sea and Okhotsk Sea is smaller and wave length is shorter. As a result linearity of the magnetic anomalies is less obvious, compared with that in the Pacific.

The marginal seas, which are situated on the continental side of island arcs, have their own characteristics which are in many ways, such as in topography, heat flow and gravity fields, different from those of typical oceans (UYEDA and VACQUIER, 1968; KARIG, 1970; KARIG, 1971). Such characteristic features have been explained in terms of extensional development of basins associated with descending lithosphere under island arcs (KARIG, 1970; UYEDA and SUGIMURA, 1970; HASEBE et al., 1970; MATSUDA and UYEDA, 1971).

In this paper, the author attempts to clarify the geomagnetic characteristics of these seas based mainly on our own measurements. It is then hoped that the process of evolution of the marginal seas and plate tectonics in the northwestern Pacific are discussed. The GSFC (12/66) model (CAIN et al., 1967) which gives almost the same main field around Japan as IGRF is used as the reference field in this study.

2. Data Reduction

2–1. Data

The magnetic data used in this study, i.e. the total intensity of the earth's filed, were punched, together with other informations such as date, time, location, sea depth and cruise name, in a few hundred thousand cards. The ship's tracks are

shown in Fig. 1. The total intensity of the earth's magnetic field was measured in almost all the cases by proton-precession magnetometers. Ship's positions were determined by the LORAN system (LORAN-A and LORAN-C), star fixes and recently by the satellite navigation system.

Through the improvements in the magnetometer and by the advent of satellite navigation system, the accuracy has recently been improved to one gamma in the total intensity and a few hundred meters in ship's position. But much of the data do not have such an accuracy. The data obtained in the earlier period sometimes carried errors of a few tens of gammas in the total intensity and rough weather or poor network of the LORAN system often did not allow one to determine the ship's position any better than a few miles.

Magnetic anomalies were calculated by removing GSFC (12/66) (Goddard Space Flight Center, December, 1966) field from the observed values of the total force, and plotted on the map by Mercator projection along ship's tracks. These processes

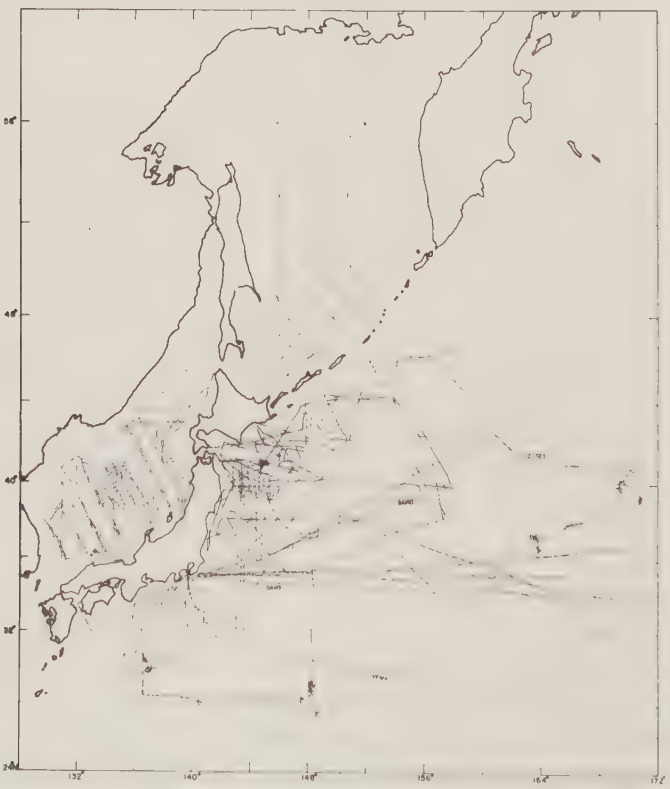

Fig. 1. Track chart. Tracks in the Japan Sea are presented in the bottom figure.

were done by a digital and a analogue computer. Total intensity and its anomaly distributions were represented as contour lines drawn by hand.

2–2. Reference Geomagnetic Field

The usual way to get a reference geomagnetic field is to construct a normal distribution of the magnetic field in the survey area. A normal distribution is expressed by the method of least squares using a simple function such as a polynomial or a Fourier series. Magnetic anomalies are defined as deviation from the constructed normal distribution. The main defect of this method is that the trend of a normal distribution is effective only in the particular survey area and can not be extended outside the area. Moreover it is difficult to construct a normal distribution where the track lines are sparse.

So, there had been increasing requests by magnetic analysts, studying large

scale tectonics, for one standard reference geomagnetic field which should satisfy the following main requirements: the field can be applied anywhere and anytime and the field is sufficiently smooth so that longer scale regional anomalies can be seen. To meet these requirements, it is considered that a smoothed field obtained from the results of magnetic observations all over the world has to be the reference field. The simplest method of producing a smoothed field over the world is to fit the observations by a series of spherical harmonics. This has been done by several authors (e. g. NAGATA and OGUTI, 1962; LEATON et al., 1965; CAIN et al., 1965; HURWITZ et al., 1966) and some of these fields in environs of Japan are shown in Fig. 2. In these fields GSFC (12/66) model matches best with the actual field because of the great amount of magnetic data used. As shown in Fig. 2, the U.S. Hydrographic Office, Chart No. 1703–field fits neither the absolute value nor the trend of the actual field. UYEDA et al., (1967) and YASUI et al., (1967, 1967) had to make some artificial adjustments in obtaining the magnetic anomalies for they chose this field as the reference field. In 1968, IAGA (International Association of Geomagnetism

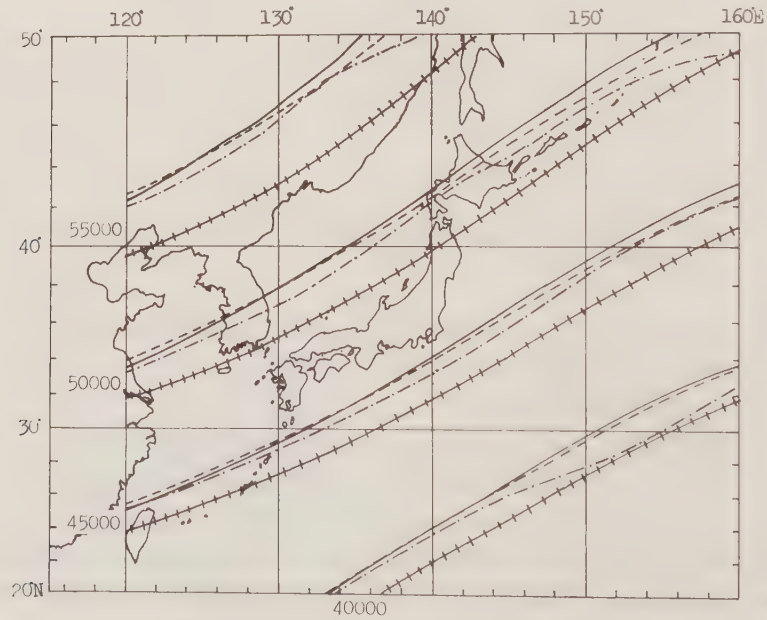

Fig. 2. Reference Fields. (in gammas)
——— GSFC (12/66)
HURWITZ et al.
++++ LEATON et al.
-·-·-·- U.S. Hydrographic Office Chart No. 1703

and Aeronomy) Comission 2 Working Group adopted IGRF (International Geomagnetic Reference Field) 1965, a composite of representations submitted by various authors.

GSFC (12/66) gives almost the same field as IGRF around Japan, i. e. the total intensity of IGRF is only several tens of gammas higher and the secular change of IGRF is several gammas/year lower than those of GSFC (12/66). Since 1967, our magnetic data have been adjusted by GSFC (12/66) so that for the sake of analyses, GSFC (12/66) is chosen as a reference field throughout this paper. As mentioned above, this choice of GSFC (12/66) does not cause any substantial difference from choosing IGRF in the areas concerned.

2–3. GSFC (12/66) Field

GSFC (12/66) was presented as a response to the need for an international reference field, the main geomagnetic field of internal origin (GAIN et al., 1967). This model is described by a series of 120 spherical harmonic coefficients ($n=m=10$) and their first and second time derivatives from the epoch 1960.0. It was derived from all the magnetic survey data available for the interval 1900–1964 plus a global distribution of geomagnetic field obtained by the OGO–2 satellite.

The magnetic field expressed by a spherical harmonic expansion of order and degree up to about 10 has been believed to be produced in the earth's core or the deep mantle. ALLDREDGE et al. (1961, 1963) showed that the Fourier coefficients of the round-world magnetic profile decrease in amplitude very rapidly up to order 7, beyond that the envelope of the coefficients slowly decreases, indicating the two divisions of sources of the geomagnetic field. They are, core sources and crustal sources. They confirmed that the magnetic anomalies with wave lengths shorter than about 200 miles can be assumed due to variation in crustal magnetization while those with wave lengths longer than 2000 miles are probably due to the earth's core or deep mantle effects and that the main geomagnetic field whose sources are in the earth's core should be described quite adequately by a spherical harmonic expansion of order and degree 10.

On the other hand, a spherical harmonic expansion has fundamental limitations that harmonic coefficiets contain errors stemming from the distribution and errors of the raw data, and from the mutual dependence of the coefficients. Therefore, the problems were what coefficients are reliable and how many are to be used in the series for the main geomagnetic field and in the series for the secular variation (CAIN et al., 1965, 1967; ALLDREDGE, 1965; HEIRTZLER, 1965; NAGATA, 1965; BULLARD, 1967).

NAGATA (1965) discussed about the convergence of the harmonic series based

on the analysis made by VESTINE et al. (1963) and FANSELAU and KAUTZLEBEN (1958) and suggested that the main geomagnetic field originating within the earth's core can be expressed by spherical harmonics of order lower than 8. But the recent models, that are GSFC (12/66), IGRF, and so on, present better convergence because of the greater amount and better distribution of magnetic data than those of two models in NAGATA's investigation.

The magnetic field potential V of internal origin is expressed by a spherical harmonic series as

$$V = a \sum_{n=1}^{\infty} \sum_{m=0}^{n} \left(\frac{a}{r}\right)^{n+1} [g_n^m \cos m\lambda + h_n^m \sin m\lambda] P_n^m(\cos\theta) \qquad (2\text{–}3\text{–}1)$$

where a, r, θ and λ denote respectively the earth's radius, the geocentric distance, the geographic co-latitude and longitude. In geomagnetism, the SCHMIDT's normalized surface spherical harmonic function has been customarily adopted for $P_n^m(\cos\theta)$ and g_n^m and h_n^m are the Gaussian coefficients.

The normalized amplitude a_n^m of each harmonics is

$$a_n^m = \sqrt{\frac{(g^{um})^2 + (h_n^m)^2}{2n+1}} \qquad (2\text{–}3\text{–}2)$$

and the contribution A_n of all the harmonics of order n to the field is

$$A_n = \sum_m a_n^m \qquad (2\text{–}3\text{–}3)$$

If the source of the magnetic potential which has a white spectrum of intensity A_0 is at the depth of a_0 from the geocenter, the amplitude of order n at the surface of the earth ($r=a$), that is A_n, is

$$A_n = A_0 \times \left(\frac{a_0}{a}\right)^{n+1}$$

Therefore,

$$\log A_n = n \log\left(\frac{a_0}{a}\right) + \log\left(\frac{a_0}{a} A_0\right) \qquad (2\text{–}3\text{–}4)$$

Since the second term is constant, $\log A_n$ is a linear function of order n. This is shown in Fig. 3 for the recent four models. The source depth, a_0, can be obtained from the gradient of the straight line which is equal to $\log(a_0/a)$. All of the four models show a good convergence up to about $n=10$ and give almost the same source depth, 1,000 kilometers inside the earth's core (GSFC (12/66)–2,580 km, IGRF–2,500 km,

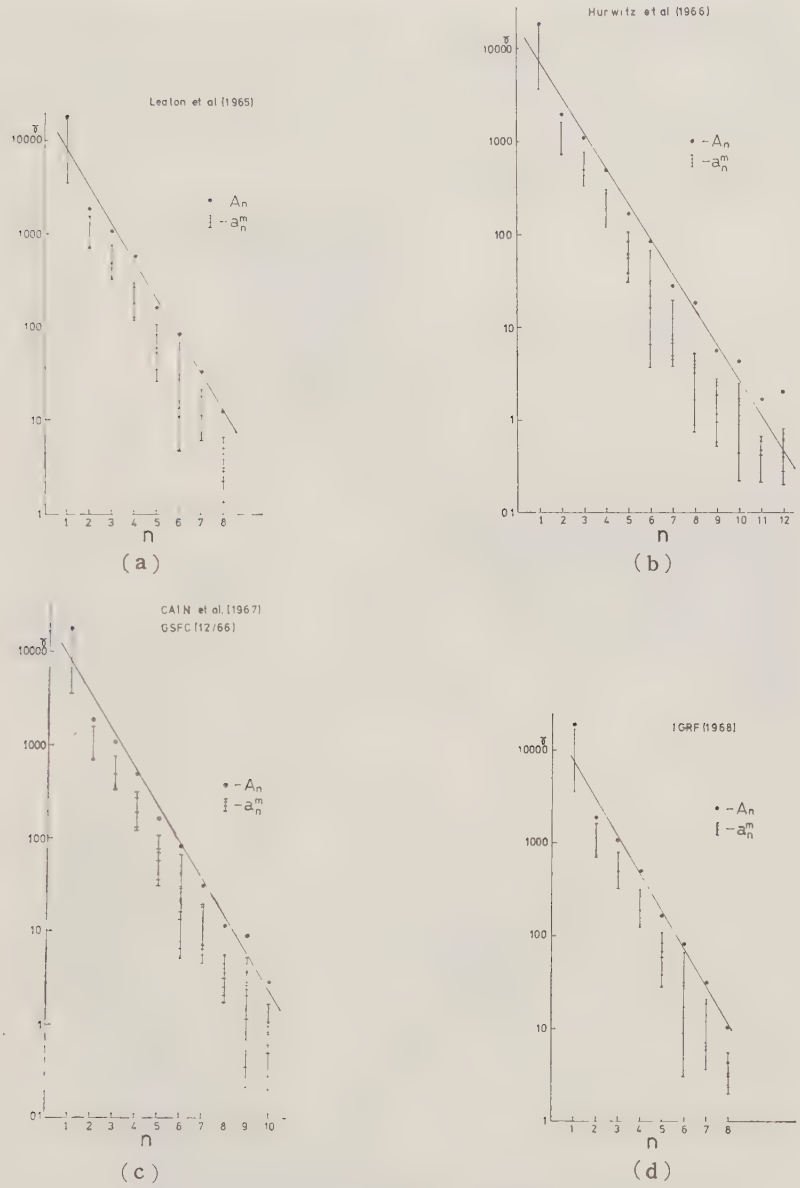

Fig. 3. $n-\log A_n$ diagram.
3a, Leaton et al. 3c, GSFC (12/66)
3b, Hurwitz et al. 3d, IGRF

LEATON et al.–2,500 km, HURWITZ et al.–2,600 km). Thus, almost all components of GSFC (12/66) can be seen to be generated in the earth's core.

2–4. Secular Change Correction

From 1964 to 1967, magnetic surveys were carried out by YASUI and others on R/V Seifu Maru in the Japan Sea (YASUI et al., 1967) and the author recompiled these data using GSFC (12/66) as a reference field (ISEZAKI, 1969, 1970), resulting in magnetic anomalies which were biased by about −100 gammas as shown in Fig.

Fig. 4. Magnetic anomaly contours in the Japan Sea by the data obtained by Seifu-maru only. Contour interval is 100 gammas.

4. In 1970, we surveyed in the Japan Basin by R/V Kofu Maru and obtained magnetic anomalies biased by about −200 gammas (ISEZAKI et al., 1971). Fig. 5 shows the magnetic anomaly profiles in the Japan Basin which show a change of the zero-level of anomalies by about −100 gammas in 5 years. GSFC (12/66) presents the total intensity in 1970 about 30 gammas larger that that in 1965 in this area. Then, the true secular change in the total intensity is considered to be about −26

Fig. 5. 5a, Track lines
..... Seifu-maru (1965)
——— Kofu-maru (1970)
5b, Magnetic anomaly profiles. Track number is referred to 5a.
5c, Magnetic lineations. Solid lines are positive anomalies and dotted lines are negative anomalies.

gammas/yr in the Japan Basin under the assumption that the secular change of the magnetization producing magnetic anomaly is negligibly small. Since the detailed magnetic survey conducted in 1970 all over the Japan Sea (see *3-2*) also resulted in a −200 gamma shift of the zero level, −26 gammas/yr appears to be the true secular change almost all over the Japan Sea.

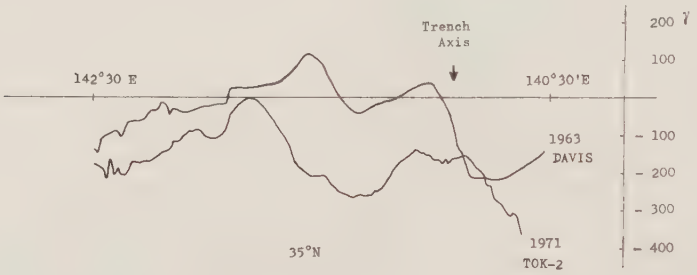

(a)

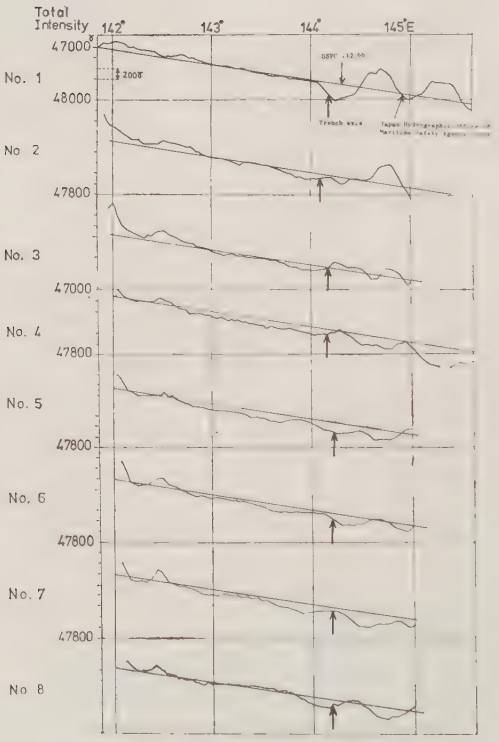

(b)

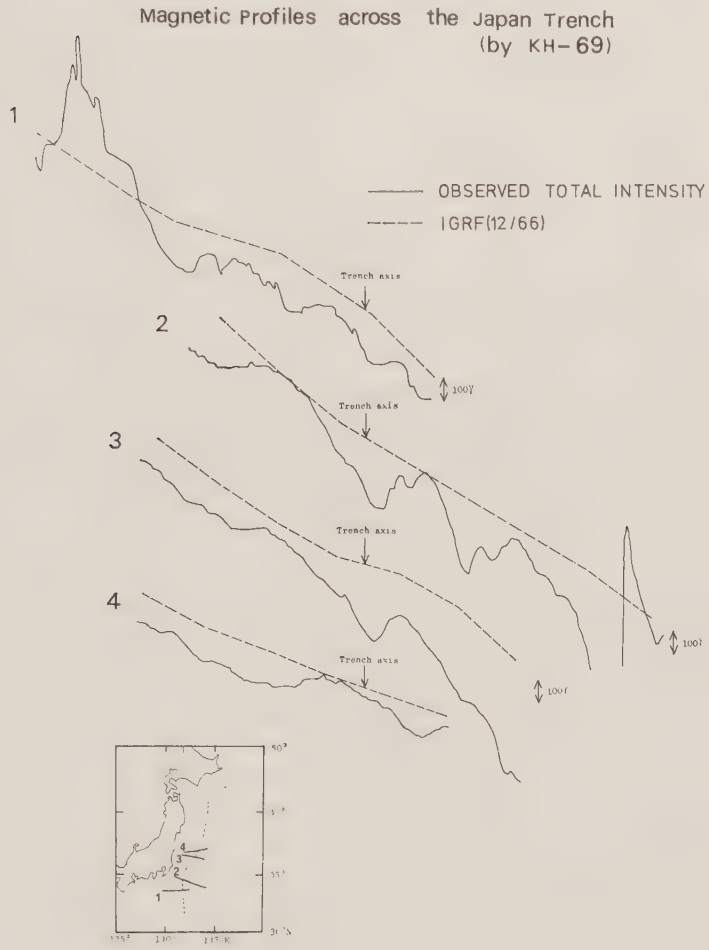

(c)

In the Pacific, R/V Davis of US Naval Oceanographic Office in 1963 and R/V Tokai-Daigaku Maru II in 1971 sailed on almost the identical track along 35°N. Their magnetic anomalies present the secular change, of about −20 gammas/yr. Other examples of the secular change in the Pacific off Honshu are shown in Fig. 6 and they give the secular change of about −23 gammas/yr.

In the Okhotsk Sea, the secular change seems to be about −25∼−30 gammas/yr, but it is still slightly uncertain because we do not have track lines which are suitable enough to estimate the secular change as shown in Fig. 7.

The observations of the total intensity by land observatories in Japan show

(d)

Fig. 6. Secular change of geomagnetic field off Honshu.
6a, Two anomaly profiles along 35°N.
6b, Magnetic profiles across the Japan trench in 1964.
6c, Magnetic profiles across the Japan trench in 1969.
6d, Magnetic profiles off Sanriku.

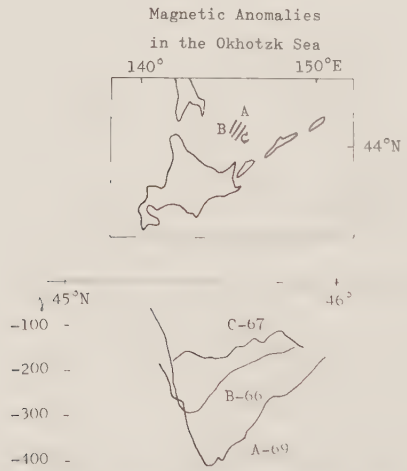

Fig. 7. Secular change of geomagnetic field in the Okhotzk Sea.

−10～−14 gammas/year during the period 1960–1965 and −20～25 gammas/yr after 1965 over the Japanese islands as the secular change (Fig. 8).

Though details of the local anomaly of the secular change in environs of Japan are unknown, it can be saide that the secular change in the total intensity is rather uniform around Japan, that is, −20～−25 gammas/yr after about 1965.

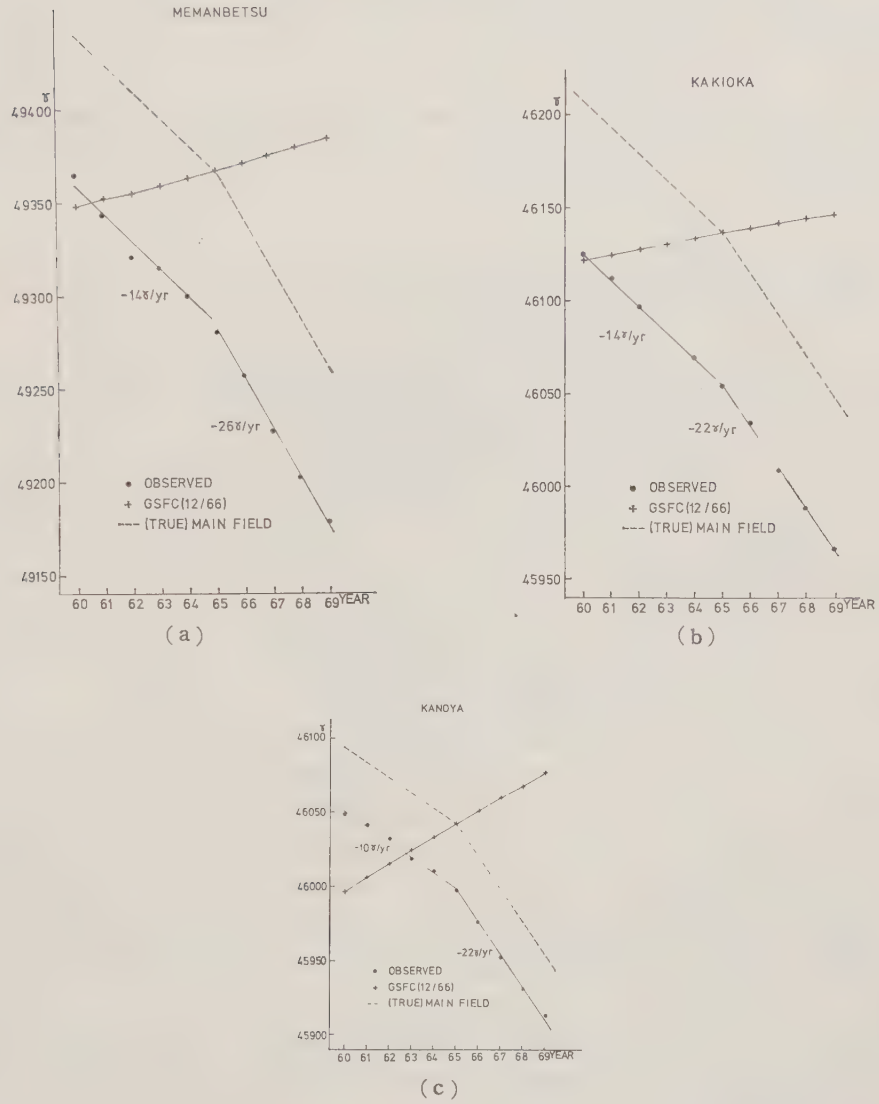

Fig. 8. Secular change of geomagnetic field on the land of Japan.
8a, Memanbetsu in Hokkaido.
8b, Kakioka in Honshu.
8c, Kanoya in Kyushu.

If −23 gammas/year is chosen as the true secular change, −25 gammas/yr becomes the secular change correction for GSFC (12/66) field throughout the area concerned in this paper, taking account of the secular change +2 gammas/yr of

GSFC (12/66). The magnetic anomaly ΔT, then, is defined as follows:

$$\Delta T = T - GSFC(12/66) - 25 \times (1965 - Y) \qquad (2\text{–}4\text{–}1)$$

where T and Y are the observed field and the year of observation respectively. (2–4–1) means that the geomagnetic main field should be identical with GSFC (12/66) field in 1965. This will be shown in 3.

3. Features of Geomagnetic Anomalies around Japan

3–1. Northwestern Pacific

Since 1961, Japanese magnetic surveys in the northwestern Pacific have been carried out mainly during cruises of JEDS (Japanese Expedition of Deep Seas).

UYEDA et al. (1967) presented the charts of the total geomagnetic intensity and its anomalies in the northwestern Pacific, compiling all the existing data at that time. As mentioned above, they chose the magnetic chart of U.S. Hydrographic Office, Chart No. 1703 for the year 1955 as their reference field. The magnetic anomalies obtained in this way were not even around zero, but were biased by about −500 gammas in the western part of the area concerned (∼135°E) and about −100 gammas at the eastern end (∼165°E) (Fig. 20).

The present author recalculated the magnetic anomalies from the same data as those of UYEDA et al. (1967), using GSFC (12/66) as the reference field and obtained a slightly different anomaly chart as shown in Fig. 9 (ISEZAKI, 1969). Fig. 9 shows that the magnetic anomaly lineations are very clearly present in the northwestern Pacific, especially in the area off the Sanriku and Hokkaido coasts and their direction is ENE-WSW, their wave lengths are 50 km to 80 km and their peak to to bottom amplitudes are 500 gammas to 1,000 gammas. These lineations are confirmed to extend at the foot of the Emperor Seamount Chain (∼170°E), changing their direction to almost E-W, by the data collected mainly by the Lamont-Doherty Geological Observatory of Columbia University (Fig. 10) (ISEZAKI, 1969). On the other side of the Emperor Seamount Chain, magnetic anomaly lineations run E-W (ERICKSON and GRIM, 1969; GRIM and ERICKSON, 1969) to the eastern Pacific off the west coasts of the north American continent, where the direction of magnetic lineations changes to N-S through the "Great Magnetic Bight" (ELVERS et al., 1967).

Fig. 11 which includes the new data after MURAUCHI et al. (1973) shows the profiles of magnetic anomaly lineations off the Hokkaido coasts. Wave lengths and amplitudes of these anomalies correlate well with each other. It is distinct from

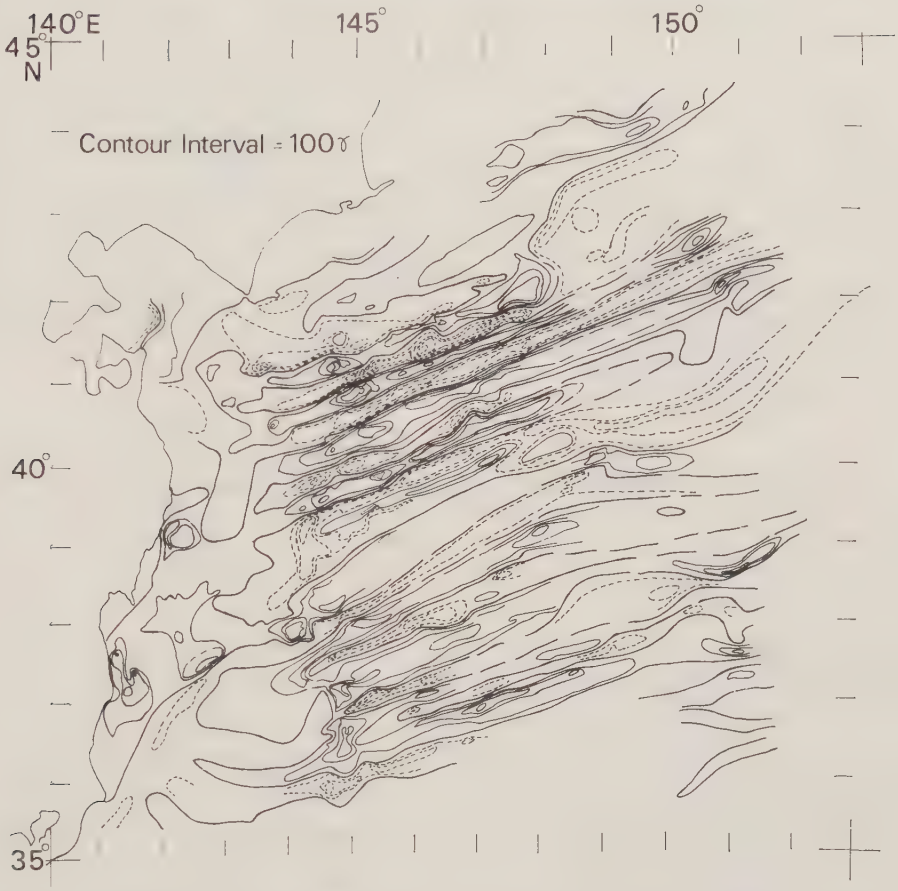

Fig. 9. Magnetic anomaly contours off the coast of Sanriku and Hokkaido. Solid lines represent positive anomalies and broken lines represent negative anomalies.

Figs. 6, 9 and 11 that amplitudes decrease abruptly just above the trench axis and the area between the trench axis and the Japanese islands is magnetically calm (~100 gammas). Magnetic anomaly lineations fade away soon in the zone of 20–40 km beyond the trench axis to the Japanese islands (Figs. 6 and 11). It appears from these facts that the origin of magnetic anomalies becomes progressively deeper toward the islands.

The area of Figs. 9, 10 and 11 is the northwestern Pacific basin where the water depth is 5,000 m to 6,000 m. In the adjacent area south of the northwestern Pacific basin, enclosed by the Hawaiian islands, the Marcus-Necker ridge and the Shatzky

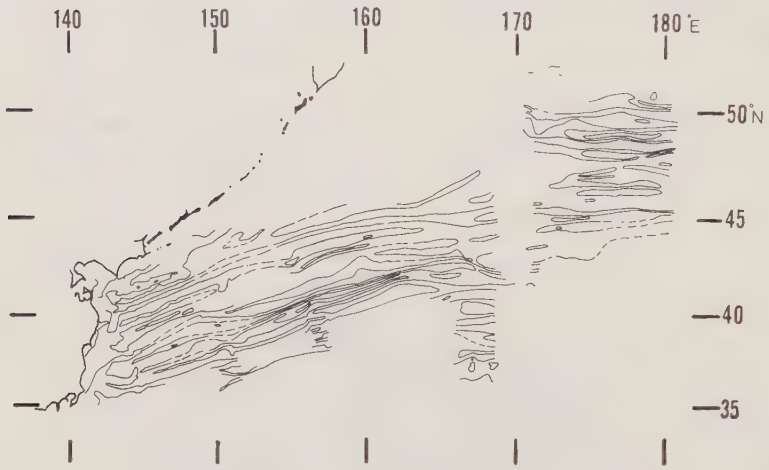

Fig. 10. Magnetic anomaly lineations in the northwestern Pacific.

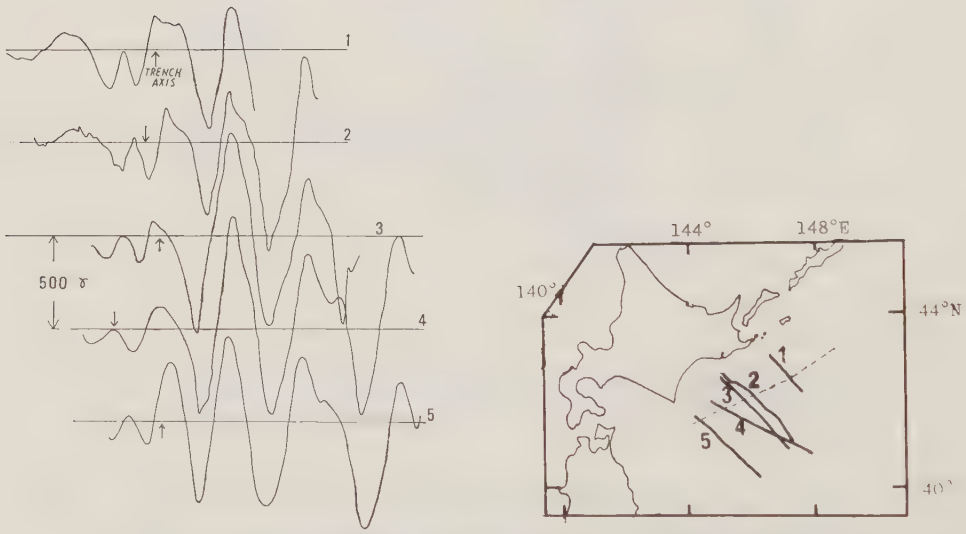

Fig. 11. Profiles of magnetic anomaly lineatons off the Hokkaido coasts.

Rise, where the water depth is also 5,000 m to 6,000 m, magnetic anomalies are quite different from those in the northwestern Pacific basin (ISEZAKI, 1969; HAYES and PITMAN, 1970). The peak to bottom amplitudes are 300 to 400 gammas and the trend of magnetic anomaly lineations is NW-SE, being almost perpendicular to the trend in the northwestern Pacific basin. A schematic map of magnetic anomalies in the north Pacific is shown in Fig. 12 (ISEZAKI, 1970), which suggests the pre-

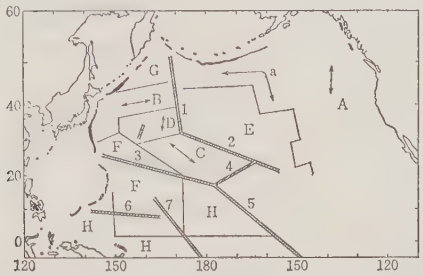

Fig. 12. Schematic Map of the Distribution of Magnetic Anomalies in the North Pacific.
A, B, C, D: Regions having the magnetic anomaly lineations (The arrows indicate the direction of lineations).
H: Region having the large magnetic anomalies but not known lineations.
E, F, G: Magnetic Quiet Zone.
1: Emperor Seamount Chain 2: Hawaiian Ridge 3: Marcus Wake Seamount Chain 4: Wake Necker Ridge 5: Christmas Ridge 6: Caroline Islands 7: Marshall Islands, Gilbert Islands a: Great Magnetic Bight

valence of more complicated tectonics in the nothwestern Pacific than in the eastern Pacific. Thanks to the cooperative program between Scripps Institution of Oceagraphy, University of California, and our group, the magnetic data obtained by Scripps scientists have been made available in the northwestern Pacific, so that we can establish more reliable configulations of the distribution of magnetic anomaly lineations. This work is being carried out through a successful cooperation to construct the tectonic history of this important area (HILDE et al., in preparation). (See 5).

3-2. Japan Sea

As mentioned already in 2, YASUI and his colleagues of Maizuru Marine Observatory made magnetic surveys from 1964 through 1967 aboard R/V Seifu Maru in the Japan Sea. They made a magnetic anomaly chart of this sea by the same method as that of UYEDA and others (1967) and presented the existence of elongated anomalies whose linearity was less distinct than that of the northwestern Pacific basin (YASUI et al., 1967). The author in 1969 recompiled the same data using GSFC (12/66) as a reference field, but it was found impossible to complete the magnetic anomaly chart because the amplitudes were too small and wavelengths were too short to be contoured with the available data. Because of the possible importance of magnetic anomalies in the tectonics of the Japan Sea, we decided in 1970 to carry out intensive surveys to fill the magnetically blank areas in the Japan Sea. At

first, in May 1970, a magnetic survey of closely spaced tracks was carried out by R/V Kofu Maru of Hakodate Marine Observatory in the eastern part of the Japan Basin. It was found that low amplitude (~100 gammas) and short wavelength (20~40 km) linear magnetic anomalies do exist in the basin (ISEZAKI et al., 1971), (Fig. 4). The second but more extensive survey was carried out by a chartered fishing boat, Daiei Maru No. 83 (193 gross tonnage), in which we brought the instruments necessary for the survey, that were, a proton-magnetometer, towed acoustic tranceiver and its recorder borrowed from Dr. G. SHOR, Scripps Institution of Oceanography, a Loran receiver and so on. We had to build a tiny hut on the tail deck of the boat to house the instruments and to make observations.

(a)

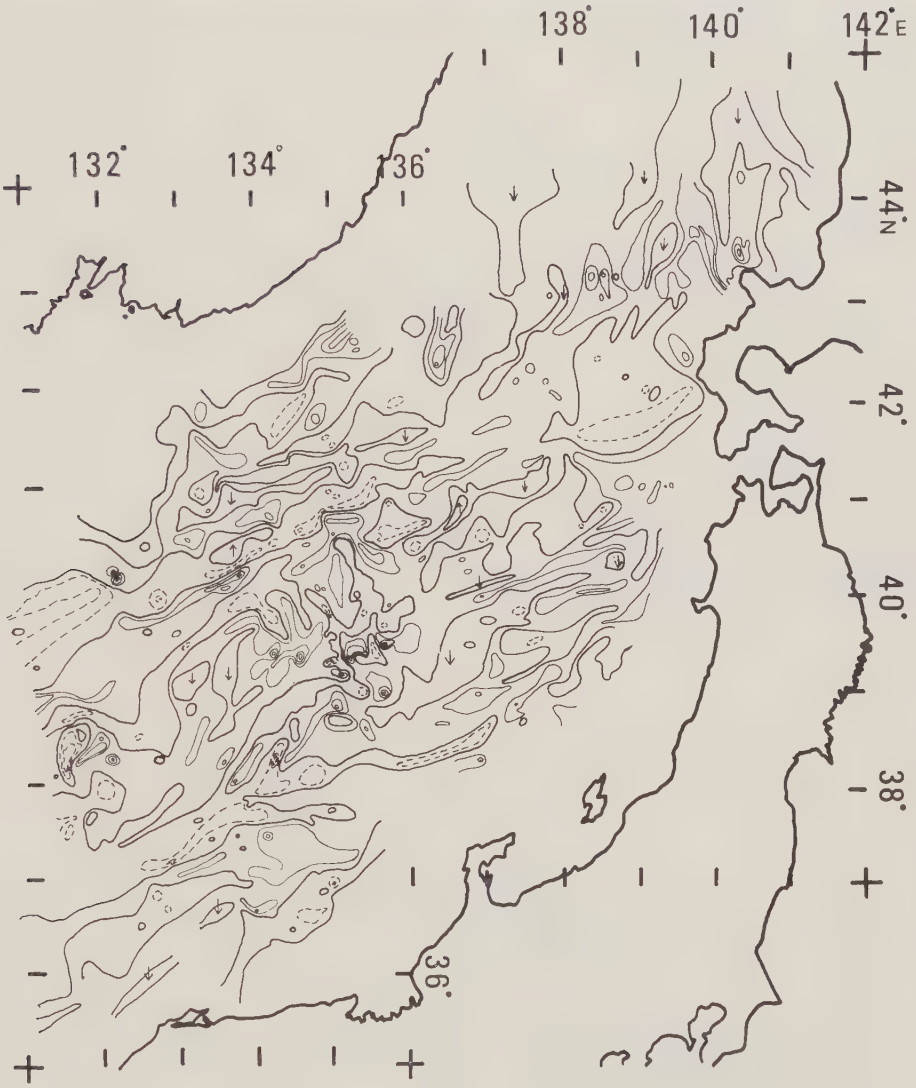

(b)

Fig. 13. Magnetic contours in the Japan Sea made by all available data so far.
13a, Total intensity contors in 1970. Contour interval is 100γ.
13b, Total intensity anomaly contours. −100γ DC component is removed. Contour interval is 100γ. Solid lines represent positive anomalies and broken lines represent negative anomalies. Thick solid lines represnt 0γ.

The results are presented in Fig. 13, in which data obtained by the Hydrograpic Office of Japan Maritime Safety Board and Ocean Research Institute of University

of Tokyo are also incorporated (ISEZAKI and UYEDA, 1973). By the definition of the total intensity anomaly (2–4–1) all anomalies in the Japan Sea are biased by about −100 gammas. On the other hand, in the Pacific, magnetic anomalies defined by (2–4–1) are balanced about the zero level as shown in Figs. 6, 9, 10 and 11. Fig. 14 represents the total intensity distribution for the epoch 1965 after UYEDA et al. (1967) and the GSFC (12/66) field is almost identical with the absolute values and the trend of the observed total intensity in this area. This is the main reason why the year 1965 is taken as the time origin of the secular change correction in (2–4–1). The feature is more clearly represented in Figs. 15 and 16. Fig. 15 shows the normal distribution of the total intensity for 1965 derived from the observations of 40 land magnetic stations and aeromagnetic surveys over the seas close to the coasts of the Japanese islands (MATSUZAKI, 1968). The GSFC (12/66) field for 1965 well fits the observed distribution except for the Hokkaido district where the fit is poor due to inadequate quantity of magnetic data and large magnetic anomalies. Fig. 16 is the result of WMS (World Magnetic Survey) in Japan (1966) which also agrees with the GSFC (12/66) field on the land and the seas except for the Japan Sea. Fig. 17 shows the total intensity distribution in the Japan Sea in 1965 after

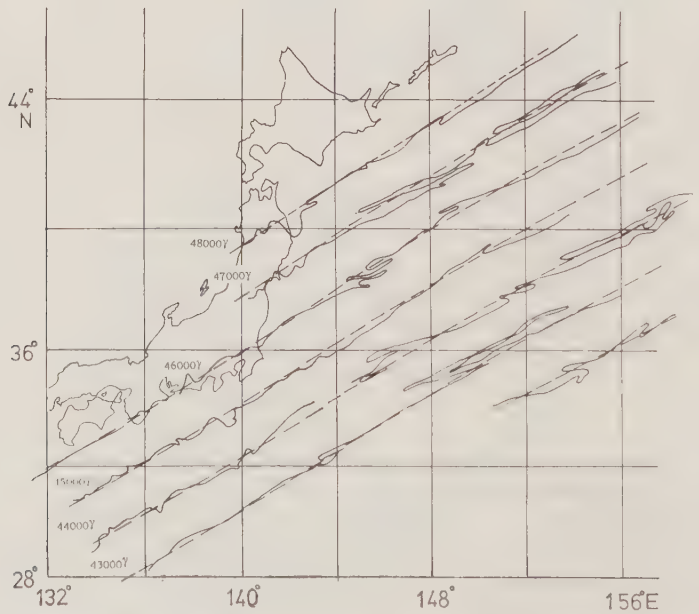

Fig. 14. Observed total intensity distribution (solid line) and GSFC (12/66) (broken line) in the northwestern Pacific and the Shikoku Basin in 1965.

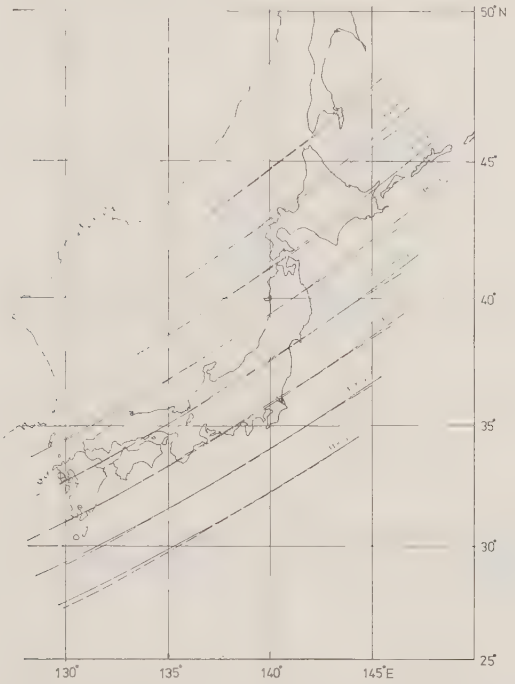

Fig. 15. Normal distribution of the total intensity obtained from the observations by Japan Hydrographic Office (solid line) and GSFC (12/66) (broken line) in 1965.

YASUI et al. (1967) and the GSFC (12/66) field. The observed fields are systematically lower than the GSFC (12/66) field by about 100 gammas.

Summarizing the above findings, it may be concluded that the GSFC (12/66) field for 1965 agrees well with the observed field in the areas, that are, the northwestern Pacific, the Shikoku Basin and the land of Japan, but does not fit the observations in the Japan Sea by about 100 gammas. This means that the magnetic anomalies in the Japan Sea have a DC component of about −100 gammas. In Fig. 18, the isodynamic line of the total intensity 48300γ for 1965 which runs through the Pacific, the land of Japan and the Japan Sea, shows a discrete northwestward displacement at the margin of the Japan Sea. There seems to be no change in the direction of the line. In other words, the gradient of the field of the total intensity in the Japan Sea is the same as that in the adjacent areas but the absolute values are less by about 100 gammas. In Fig. 19, the magnetic profiles on the tracks C–D, E–F and G–H show this phenomenon. On the profile C–D, magnetic anomalies in

Fig. 16. Observed total intensity distribution by the WMS project (solid line) and GSFC (12/66) (broken line) in 1965.

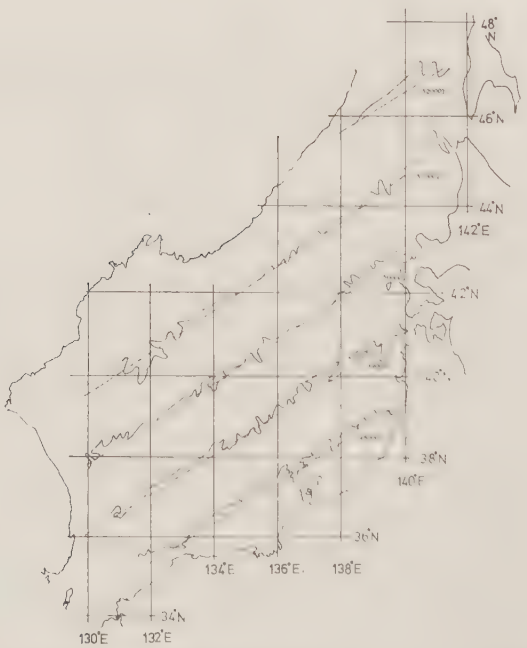

Fig. 17. Observed total intensity distribution in the Japan Sea (solid line) and GSFC (12/66) (broken line) in 1965.

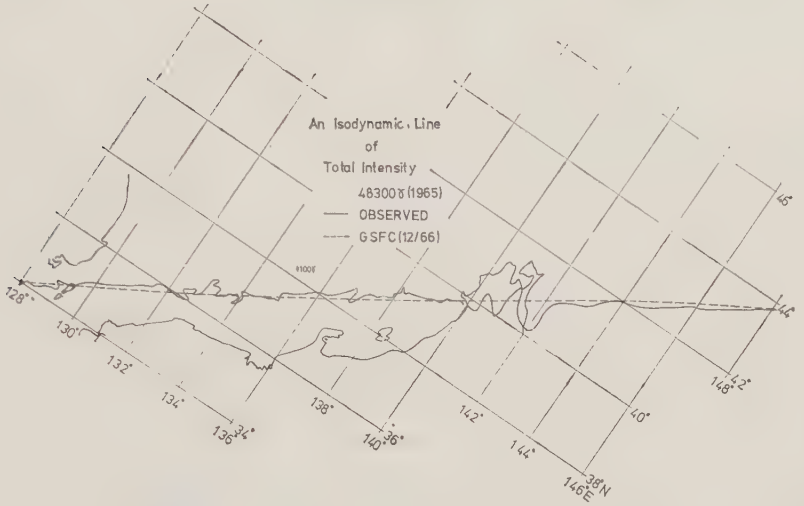

Fig. 18. The isodynamic line of 48300γ in 1965.

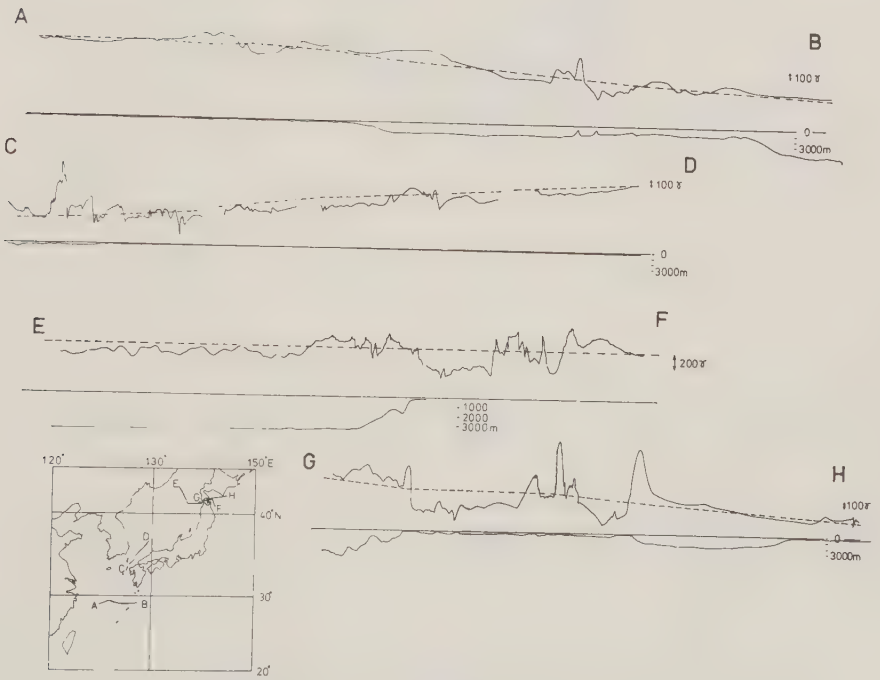

Fig. 19. Magnetic profiles indicating the DC component of −100γ in the Japan Sea.

the area between Korea and Kyushu are large and their zero level is in accordance with GSFC (12/66) and after crossing the strait of Thushima into the Japan Sea anomalies are about −100 gammas. The left side of the profile E–F shows the anomalies in the Japan Basin all of which are negative (about −100 gammas) and very large anomalies through the strait of Tsugaru. The field agrees with GSFC (12/66) in the Pacific off the Hokkaido coasts as shown in the profile G–H. In Fig. 13, magnetic anomalies are computed by eliminating this bias of −100 gammas and the total intensities are reduced to the values in 1975 through correction of the secular change. Generally speaking, magnetic anomalies in the Japan Sea are calm, even on the seamounts and their wave lengths are short compared with those in the Pacific. The directions of linearity of the magnetic anomalies are generally ENE–WSW but their features are less obvious than in the Pacific. The relatively large amplitudes or magnetic anomalies correspond to the seamounts and bathymetric uprifts, such as Yamato-Tai, and a highly magnetically disturbed zone exists, off the peninsula of Noto (about 37°30′N, 136°E) where the magnetic anomalies are so large and complicated that contouring of anomalies is not possible at the present stage. The direction of lineality of magnetic anomalies changes from ENE–WSW to N–S off the Hokkaido coasts in a fashion more or less parallel with the trend of the Japan are (ISEZAKI et al., 1971; ISEZAKI and UYEDA, 1973).

3–3. Other seas

In the Okhotsk Sea, YASUI and others made magnetic surveys in 1966 and 1967 (YASUI et al., 1968). The U.S. Hydrographic Office Chart No. 1703 for the epoch 1965 was adopted as a reference field and magnetic anomalies of −400∼−600 gammas were obtained in the southern part of the Okhotsk Sea (in the Kuril Basin), whereas those of −800∼−1,000 gammas were found in the northern part (Fig. 20). The present author also recompiled the same data by adopting the GSFC (12/66) field as a reference field and got the chart of magnetic anomalies more or less similar to that obtained by SOLOV'YEN and GAINANOV (1963) which is rather different from that of YASUI et al., (ISEZAKI, 1968) (Fig. 21). Fig. 21 shows that the amplitudes of magnetic anomalies are generally small (∼100 gammas) but some strong positive anomalies are present on the slopes between the Kuril Basin (∼3,300 m) and the An Rise (∼1,500 m). In other areas of the Okhotzk Sea the magnetic anomalies are negatively biased by about −100 gammas just as is the case in the Japan Sea. The abrupt change to the negatively biased magnetic anomalies in the Okhotzk Sea is represented by the magnetic anomaly profile across the Kuril arc from the Pacific to the Kuril Basin Fig. 22. The similar characteristics of magnetic anomalies

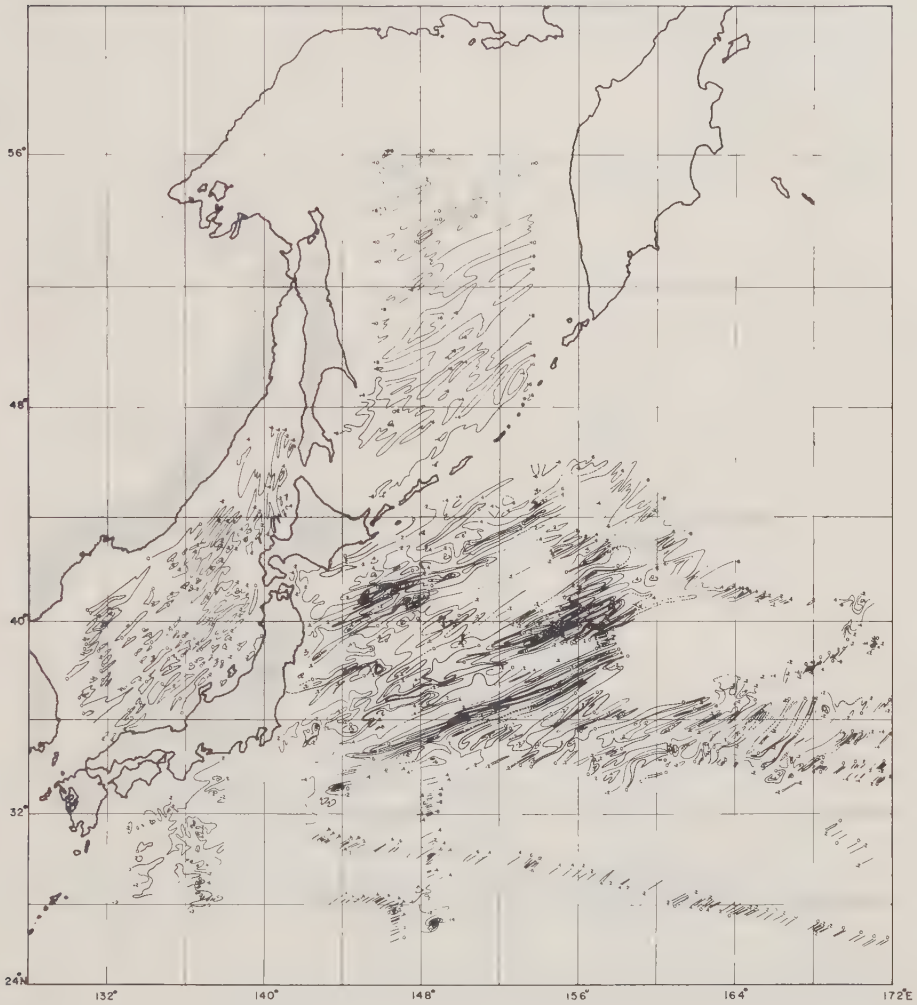

Fig. 20. Magnetic anomaly contours by UYEDA et al., (1967). U.S. Hydrographic Office Chart No. 1703 for 1955 was taken as the reference field. Unit is 100γ.

may imply similar process of evolution of the Japan Sea and Okhotzk Sea.

WAGEMAN et al. (1970) presented the magnetic anomalies in the Yellow Sea and the East China Sea (Fig. 23). Though they calculated the anomalies using IGRF as a reference field without the secular change correction, we can see a relative shift of the zero level of magnetic anomalies in these areas also, namely about −150 gammas shift of the zero level in the Yellow Sea and about −100 gammas shift in the East China Sea.

In the Ryukyu Basin, a profile A–B in Fig. 19 shows no such distinct shift of the zero level. We also could not find the systematic shift to the negative anomalies

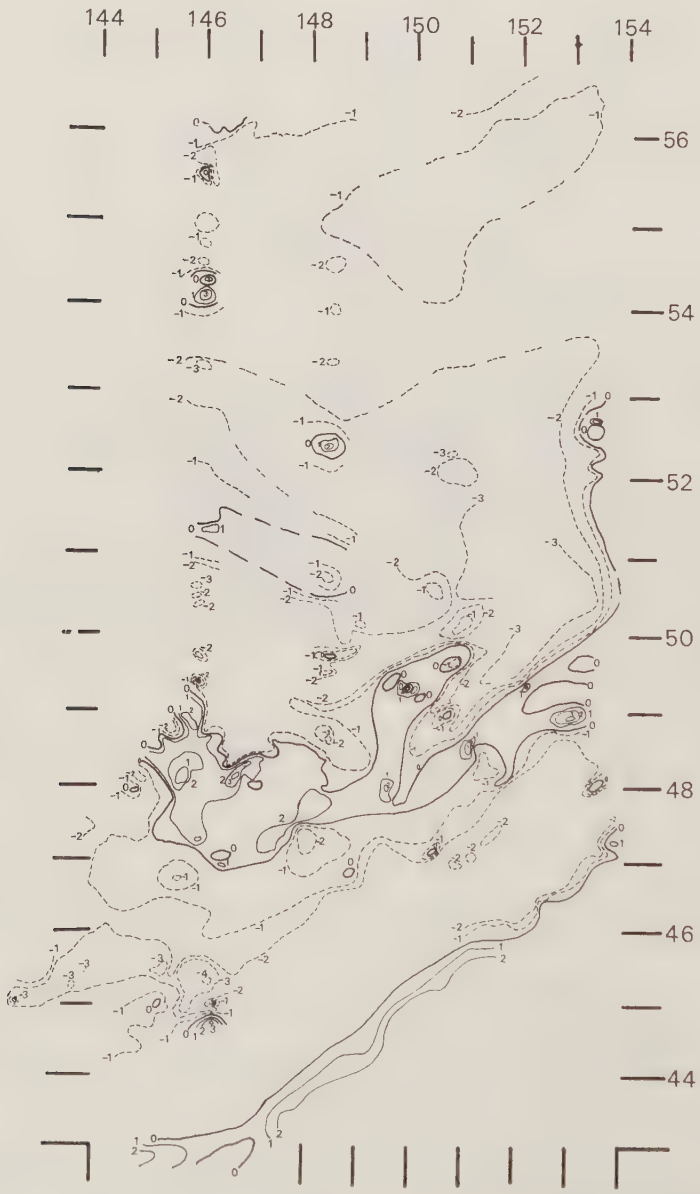

Fig. 21. Magnetic anomaly contours in the Okhotzk Sea. Unit is 100γ.

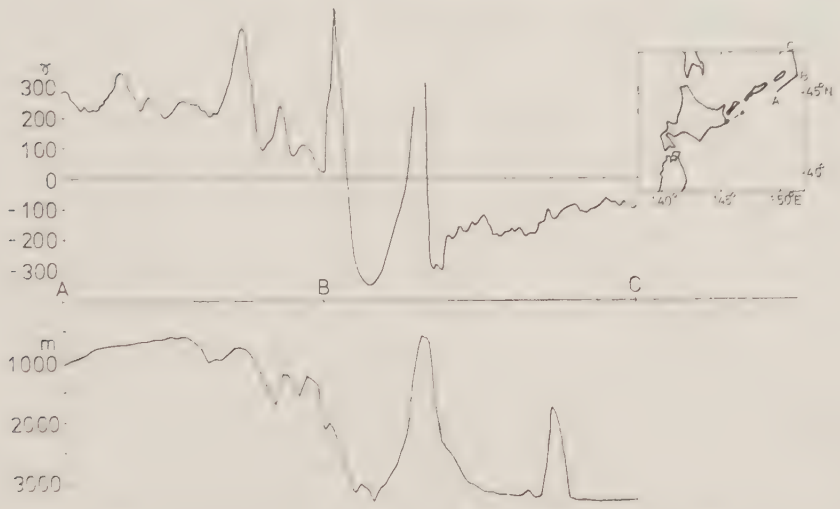

Fig. 22. A magnetic anomaly profile across the Kuril arc.

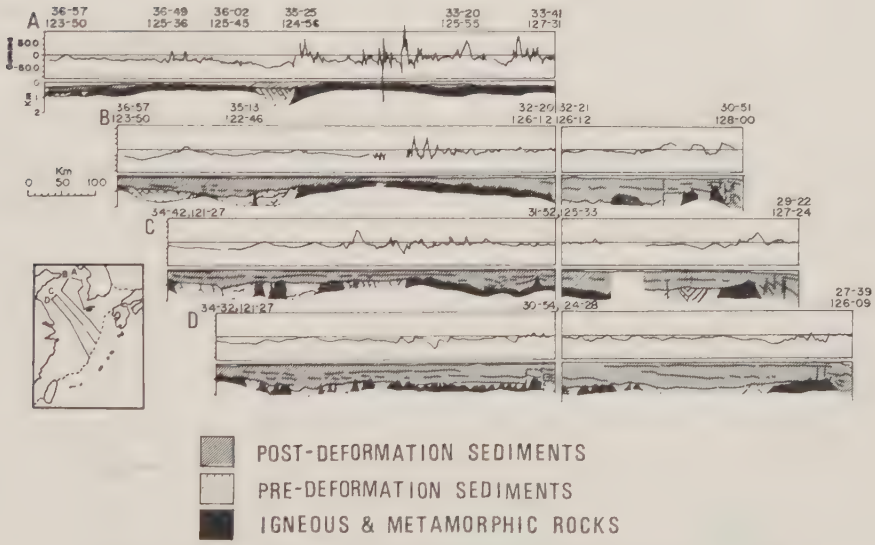

Fig. 23. Magnetic anomaly profiles in the Yellow Sea and the East China Sea by WEGEMAN et al., (1970).

in the Ryukyu Basin in 1970 (by Daiei-maru No. 83). This lack of distinct shift in the Ryukyu Basin might be related to the fact that the Ryukyu Basin is so narrow that magnetic anomalies are influenced by anomalies caused by the adjacent structures.

4. Interpretations of Magnetic Anoamlies

4–1. Method of Interpretation

Magnetic anomalies are uniquely obtained if we know the shape, the location and the magnetization (as a vectorial quantity) of the source body producing them, but it is very difficult to know uniquely the information of the magnetic source from observed magnetic anomalies.

There are two main ways to interpret magnetic anomalies; one is the harmonic analysis method and the other is to approximate the linear integral equation by a summation, namely by a set of linear equations. The former is the classical way which has been used to derive, in most cases, a two-dimentional magnetic version of the horizontal "equivalent" layer or surface on which the magnetic moments of specified direction are coated to construct the measured magnetic anomalies (e. g. NAGATA, 1938; BOTT, 1967; SEGAWA, 1967). The distribution of the magnetization obtained from this method can be converted to the surface relief of the source body (HAHN, 1965). The harmonic analysis always needs the assumption of the direction of magnetization usually taken parallel with the present geomagnetic field and the depth of the horizontal "equivalent" layer. Therefore this method gives only the magnitude of magnetization with a sign.

The latter method of interpretation is more versatile because it can be applied to irregularly shaped bodies such as a seamount, and the obsrved magnetic anomalies need not be on the same horizontal plane. Moreover, the assumption of specified direction of magnetization is not necessary.

VACQUIER (1963) and TALWANI (1965) calculated the magnetization of seamounts by this method under assumption that a seamount is uniformly magnetized. BOTT (1967) and EMILIA and BODVARSSON (1969) applied this method to interprete magnetic anomaly lineations under the assumption of the fixed direction of magnetization. Generally speaking, however, there is no good reason for the source body to be magnetized in a specified direction such as that of the present local geomagnetic field. Especially when we take into account of the sea floor spreading and polar wandering hypotheses, such an assumption is usually inappropriate.

The present author, in this section, hopes to extend this method, in order to determine the distribution of magnetization of the source body without the assumption of specified direction of magnetization.

4–2. Formulation

A right handed coordinate system is chosen in the following formulation (Fig.

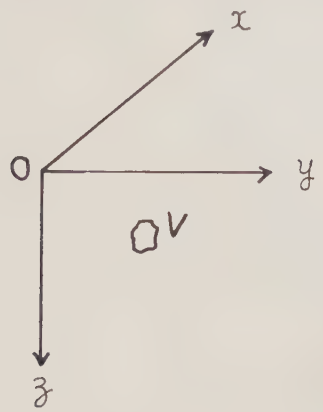

Fig. 24. Coordinate system.

24). The magnetic potential $\Omega_m(x, y, z)$ at a point (x, y, z) due to a magnetized body $V_m = \Delta\xi\Delta\eta\Delta\zeta$ which has dipole magnetization $\boldsymbol{J}_m$; $(J_{x,m}, J_{y,m}, J_{z,m})$, is experssed as follows

$$\Omega_m(x, y, z) = \frac{\boldsymbol{J}_m \cdot \boldsymbol{r}}{r^3}\Delta\xi\Delta\eta\Delta\zeta$$

$$= \frac{J_{x,m}(x-\xi) + J_{y,m}(y-\eta) + J_{z,m}(z-\zeta)}{[(x-\xi)^2 + (y-\eta)^2 + (z-\zeta)^2]^{1/2}}\Delta\xi\Delta\eta\Delta\zeta \qquad (4\text{–}2\text{–}1)$$

The x component of the magnetic field (magnetic anomaly) at (x, y, z) generated by V_m is

$$F_{x,m}(x, y, z) = -\frac{\partial\Omega_m}{\partial x}$$

$$= -\frac{\partial}{\partial x}\iiint \frac{J_{x,m}(x-\xi) + J_{y,m}(y-\eta) + J_{z,m}(z-\zeta)}{[(x-\xi)^2 + (y-\eta)^2 + (z-\zeta)^2]^{3/2}} d\xi d\eta d\zeta$$

$F_{y,m}(x, y, z)$ and $F_{z,m}(x, y, z)$ can be obtained similarly. Using the relations such as $-\partial/\partial x = \partial/\partial\xi$, $-\partial/\partial y = \partial/\partial\eta$ and $-\partial/\partial z = \partial/\partial\zeta$ and replacing variables ξ, ζ and ζ by x, y and z, the three components ΔX, ΔY and ΔZ at the origin are

$$\Delta X_m = F_{x,m}(0, 0, 0) = \iiint \frac{\partial}{\partial x}\left[\frac{J_{x,m}x + J_{y,m}y + J_{z,m}z}{(x^2 + y^2 + z^2)^{3/2}}\right] dxdydz$$

$$\Delta Y_m = F_{y,m}(0, 0, 0) = \iiint \frac{\partial}{\partial y}\left[\frac{J_{x,m}x + J_{y,m}y + J_{z,m}z}{(x^2 + y^2 + z^2)^{3/2}}\right] dxdydz$$

$$\Delta Z_m = F_{z,m}(0, 0, 0) = \iiint \frac{\partial}{\partial z}\left[\frac{J_{x,m}x + J_{y,m}y + J_{z,m}z}{(x^2 + y^2 + z^2)^{3/2}}\right] dxdydz \qquad (4\text{–}2\text{–}2)$$

Differentiating (4–2–2) with respect to x, y and z, respectively, we get

$$\begin{aligned}
\Delta X_m &= C_1 J_{x,m} + C_2 J_{y,m} + C_3 J_{z,m} \\
\Delta Y_m &= C_2 J_{x,m} + C_4 J_{y,m} + C_5 J_{z,m} \\
\Delta Z_m &= C_3 J_{x,m} + C_5 J_{y,m} + C_6 J_{z,m}
\end{aligned}$$

where

$$\begin{aligned}
C_1 &= \iiint \frac{-2x^2 + y^2 + z^2}{(x^2 + y^2 + z^2)^{5/2}} dxdydz \\
C_2 &= \iiint \frac{-3xy}{(x^2 + y^2 + z^2)^{5/2}} dxdydz \\
C_3 &= \iiint \frac{-3xz}{(x^2 + y^2 + z^2)^{5/2}} dxdydz \\
C_4 &= \iiint \frac{x^2 - 2y^2 + z^2}{(x^2 + y^2 + z^2)^{5/2}} dxdydz \\
C_5 &= \iiint \frac{-3yz}{(x^2 + y^2 + z^2)^{5/2}} dxdydz \\
C_6 &= \iiint \frac{x^2 + y^2 - 2z^2}{(x^2 + y^2 + z^2)^{5/2}} dxdydz
\end{aligned} \qquad (4\text{–}2\text{–}3)$$

The triple integrations in (4–2–3) were carried out analytically by the author for the determination of magnetization of seamounts in two cases; V_m is a rectangular prism and a polygonal lamina (ISEZAKI et al., 1972, in preparation). If $\boldsymbol{J}_m$ is assumed to be constant over all the source body (a seamount), the case of a rectangular prism almost coincides with VACQUIER's method (1962) and the case of a polygonal lamina corresponds to TALWANI's method (1965) in which he did a double integration analytically and a single integration numerically.

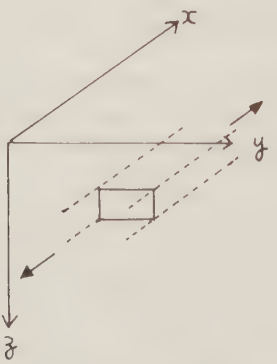

Fig. 25. The block model.

As mentioned already, in the Japan Sea and the northwestern Pacific, elongated linear anomalies are present while the topography of the sea floor doesn't have corresponding features. In these regions, we can assume the existence of elongated or lineated subterranean magnetic structures and for the interpretation of these magnetic structures two dimensional rectangular blocks extending infinitely in the direction parallel with the strike of lineations, can be adopted as the simplest case. In such a case (4–2–3) results in the following expression, in which it is assumed that the block (V_m) extends infinitely in the direction of x-axis (Fig. 25).

$$\begin{aligned} \Delta X_m &= 0 \\ \Delta Y_m &= C_4 J_{y,m} + C_5 J_{z,m} \\ \Delta Z_m &= C_5 J_{y,m} + C_6 J_{z,m} \end{aligned}$$

where

$$\begin{aligned} C_4 &= \left(\tan^{-1}\frac{z_1}{y_1} - \tan^{-1}\frac{z_2}{y_1} + \tan^{-1}\frac{z_2}{y_2} - \tan^{-1}\frac{z_1}{y_2}\right) \times 2 \\ C_5 &= \log \frac{(y_1^2 + z_1^2)(y_2^2 + z_2^2)}{(y_2^2 + z_1^2)(y_1^2 + z_2^2)} \\ C_6 &= -C_4 \end{aligned} \qquad (4\text{–}2\text{–}4)$$

y_1, y_2, z_1 and z_2 are the coordinates of the corner points of the block ($y_2 > y_1$, $z_2 > z_1$). The geomagnetic total intensity is calculated by the vectorial summation of the main earth's field, i. e. GSFC (12/66) and the anomaly expressed in (4–2–4). Then, the total intensity anomaly ΔT_m caused by V_m is represented as

$$\begin{aligned} \Delta T_m = {} & [(X + \Delta X_m)^2 + (Y + \Delta Y_m)^2 + (Z + \Delta Z_m)^2]^{1/2} \\ & - [X^2 + Y^2 + Z^2]^{1/2} \end{aligned} \qquad (4\text{–}2\text{–}5)$$

where X, Y and Z are x, y and z component of the main field (GSFC [12/66]).

The scalar intensity of magnetic anomaly $\Delta T(=(\Delta Y_m{}^2 + \Delta Y_m{}^2 + \Delta Z_m{}^2)^{1/2})$ is usually very small compared with that of the main field $T(=(X^2 + Y^2 + Z^2)^{1/2})$. Even on a strongly magnetic seamount, it is usual that $\Delta T/T < 1/50$. Therefore, the direction of the total intensity can be taken as the same as that of the main field within 1°. So, using the inclination I and the declination D of the main field, (4–2–5) is approximated well within a few gammas error by the next expression.

$$\Delta T_m = \{\Delta X_m \sin(C - D) + \Delta Y_m \cos(C - D)\} \cos I + \Delta Z_m \sin I \qquad (4\text{–}2\text{–}6)$$

where C is the angle between the geographical north and the direction of y axis measured in a clockwise direction (Fig. 26).

Substituting ΔX_m, ΔY_m and ΔZ_m in (4–2–6) by those in (4–2–4), we get

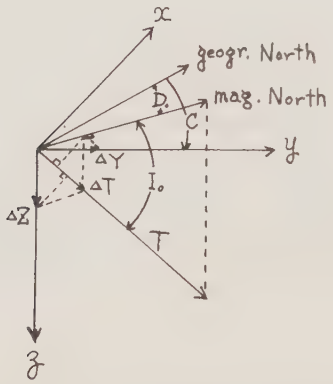

Fig. 26. The total intensity and its anomaly.

$$\Delta T_m = P_{1,m} J_{y,m} + P_{2,m} J_{z,m}$$

where

$$P_{1,m} = C_4 \cos(C - D) \cos I + C_5 \sin I$$
$$P_{2,m} = C_5 \cos(C - D) \cos I - C_4 \sin I \qquad (4\text{–}2\text{–}7)$$

The total intensity anomaly ΔT^n at a point (x_n, y_n, z_n) due to m blocks can be expressed as,

$$\Delta T^n = \sum_m [P_{1,m}{}^n J_{y,m} + P_{2,m}{}^n J_{z,m}] \qquad (4\text{–}2\text{–}8)$$

where

$$P_{1,m}{}^n = P_{1,m}(x_m - x_n,\ y_m - y_n,\ z_m - z_n)$$
$$P_{2,m}{}^n = P_{2,m}(x_m - x_n,\ y_m - y_n,\ z_m - z_n)$$

If we have $n(\geq 2m)$ observed anomalies (ΔT^n), y and z components of magnetization of each block can be determined by solving a set of n linear equations (4–2–8). The least square method is adopted ($n > 2m$) for solving (4–2–8).

4–3. Northwestern Pacific

In the northwestern Pacific, there exist some distinct magnetic anomaly lineations (Fig, 6) and a two dimensional block model is probably valid for their interpretation.

To solve (4–2–8), we have to know the configuration of two dimensional blocks. VINE and WILSON (1965) proposed that magnetization producing magnetic anomalies could be confined in Layer 2 which is supposed to be composed of 1 or 2 kilometer thick basaltic extrusive and intrusives after HESS' model of the oceanic crustal structure (1962). Though IRVING et al. (1970) and TALWANI et al. (1971) presented some evidence for the very thin thickness of the magnetic source layer i. e. 200 m

(IRVING et al.) and 400 m (TALWANI et al.) near the crestal region of the mid-Atlantic ridge, Layer 2 has been widely accepted as the source layer of magnetic anomalies in the ocean basin. In this study, Layer 2 is taken as the source layer as the first approximation.

After LUDWIG et al. (1966), Layer 2 is 6 to 8 kms below the sea level in the northwestern Pacific but we do not have sufficient seismic reflection and refraction data which can give detailed local configuration of Layer 2. Therefore, Layer 2 is assumed to be flat and horizontal in the calculation of (4–2–8).

The results are shown in Fig. 27. At a glance, the distribution of the directions

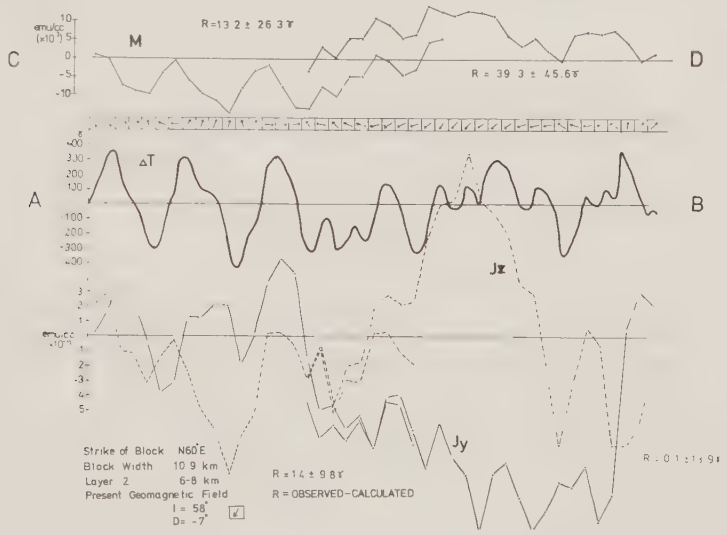

Fig. 27. Distribution of magnetization in the northwestern Pacific.

of magnetizations is rather contrary to simple intuition, namely the positive and the negative anomalies do not always correspond to the normal (parallel with the present field) and the reverse (anti-parallel with the present field) polarities of magnetizations respectively. Magnetic anomalies in the left side of the profile A–B in Fig. 27, which have a relatively simple mode, long wavelengths and large amplitudes, are represented by sudden changes of the directions of magnetizations, whereas other magnetic anomalies of the profile which have longer wavelength regional anomalies are represented by gradual changes of the directions of magnetization, of which small changes correspond to the short wavelength anomalies.

VINE and MATTHWS hypothesis (1963) assumes the specified direction of mag-

netization which is a significant restriction on (4–2–8), i. e. $P_{2,m^n}/P_{1,m^n}$=(the inclination of magnetization) constant. Fig. 27 shows that some anomalies need the abrupt change of the directions of magnetizations but the changes are not so simple as those from one direction to the opposite direction. The profile C–D in Fig. 27 is the solution of (4–2–8) under the assumption that all blocks are magnetized in the direction of the present earth's field. The profile C–D shows that the negative magnetizations (total intensity) are present in the left half of the profile. This fact is consistent with the distribution of the dominant directions nearly anti-parallel with the present earth's field as represented in the direction distribution A–B obtained under no assumption of the specified direction in Fig. 27. It is the case of the

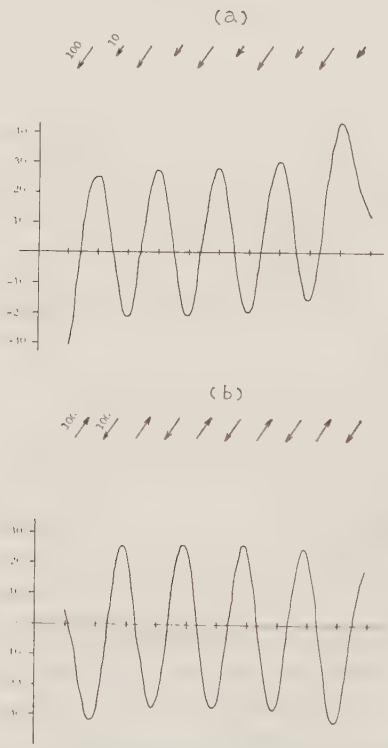

Fig. 28. Block width 10, depth 6 to 8, megnetization 100 or 10 emu/cc, parallel with the present field. Present field; I=58°, D=−7°.
28a, Magnetic anomalies produced by nomally magnetized blocks.
28b, Megnetic anomalies produced by normally and reversely magnetized blocks.

right half of the profile, almost all blcoks are magnetized in the direction of the present earth's field. This is again consistent with the direction distribution A–B. The accuracy of the solution C–D is worse than that of A–B, because of the strong restriction of the specified direction of magnetization, i. e. the residual (=observed-calculated) is 13.2 ± 26.3 gammas in C–D while -1.4 ± 9.8 gammas in A–B. Thus, it can be said that some positive-negative anomalies need sudden changes of the direction of magnetization but it does not always need the normal and reverse polarities as referred to the present earth's field. In other words, the positive and negative anomalies can be produced by magnetizations orientated to one direction. This is demonstrated in Fig. 28. After all, the present author considers that the magnetization distribution A–B should be preferable to that of C–D, because A–B is the unique solution of (4–2–8) obtained without any restricting assumptions.

The intensities of magnetizations vary from 3×10^{-3} to 1.7×10^{-2} (emu/cc) in the solution A–B and from 2×10^{-4} to 1.5×10^{-2} (emu/cc) in the solution C–D, In the reversely magnetized region there could be very rough topography corresponding to the large variation of magnetization, but we have no information about the basement topography.

4–4. Japan Sea

Layer 2 in the Japan Sea is situated at the same depth as in the northwestern Pacific i. e. 6 to 8 kms below the sea level after the seimsmic refraction data by RIKITAKE et al. (1968). The results of calculation of (4–2–8) are shown in Fig. 29. Magnetic anomalies in the Japan Sea are biased by -100 gammas and the amplitudes of fluctuations about this biased level are about 60 gammas in the profile in Fig. 30. The variation of magnetization is very small and smooth ($1.0 \sim 1.6 \times 10^{-2}$ emu/cc) due to the large amplitude of the DC component of -100 gammas compared with the fluctuation amplitude, about 60 gammas. The result that the direction of magnetizations are confined between -10 degrees and -70 degrees may be due to the fact that a unit block with the magnetization direction of -58 degrees ($+58$ degrees in the direction of the present earth's field) produces the largest negative anomaly of all directions of magnetization (Fig. 30). If the direction of magnetization is fixed in that of the present earth's field, the solution of (4–2–8) gives, as a matter of course, the reverse direction of magnetization ($1 \sim 8 \times 10^{-3}$ emu/cc) as shown in C–D in Fig. 31. This solution C–D, however, is not so good because the residual is 35 ± 50 gammas, while that of the solution (Fig. 29) A–B is 0.0 ± 2.0 gammas, as is the case of the northwestern Pacific.

If the bias of -100 gamms is eliminated and magnetic anomalies are balanced

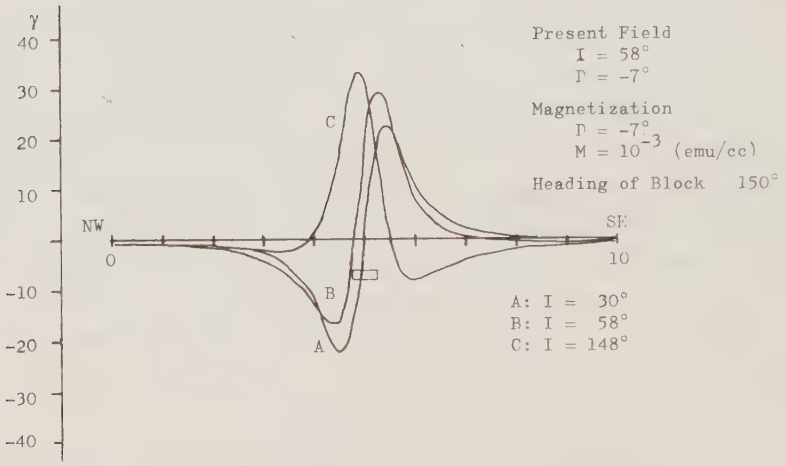

Fig. 29. Magnetic anomalies produced by magnetizations of various directions.

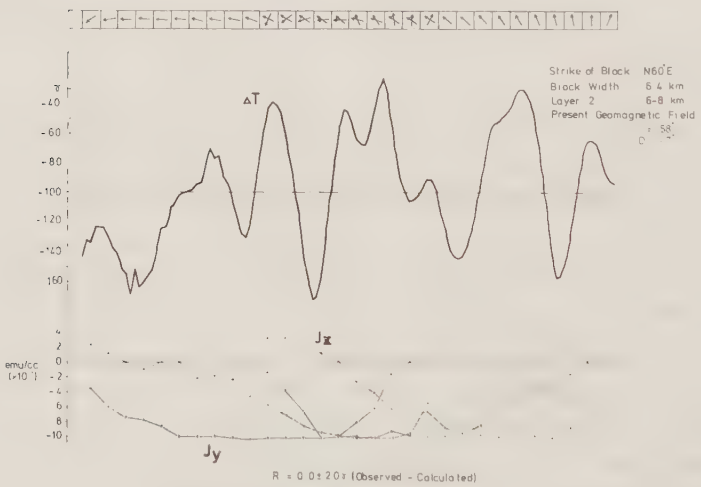

Fig. 30. Distribution of magnetization in the Japan Sea.

about the zero level, the solutions of (4–2–8) become as presented in the upper diagram of Fig. 31. Most inclinations of magnetizations are positive and their intensities range from 8.8×10^{-4} to 4.5×10^{-3} emu/cc as shown in the diagram. In the case of the fixed direction of magnetization in the present earth's field, almost all inclination are positive, i. e., parallel with the present earth's field as presented in the lower diagram of Fig. 31. This is accordant with the result of the upper

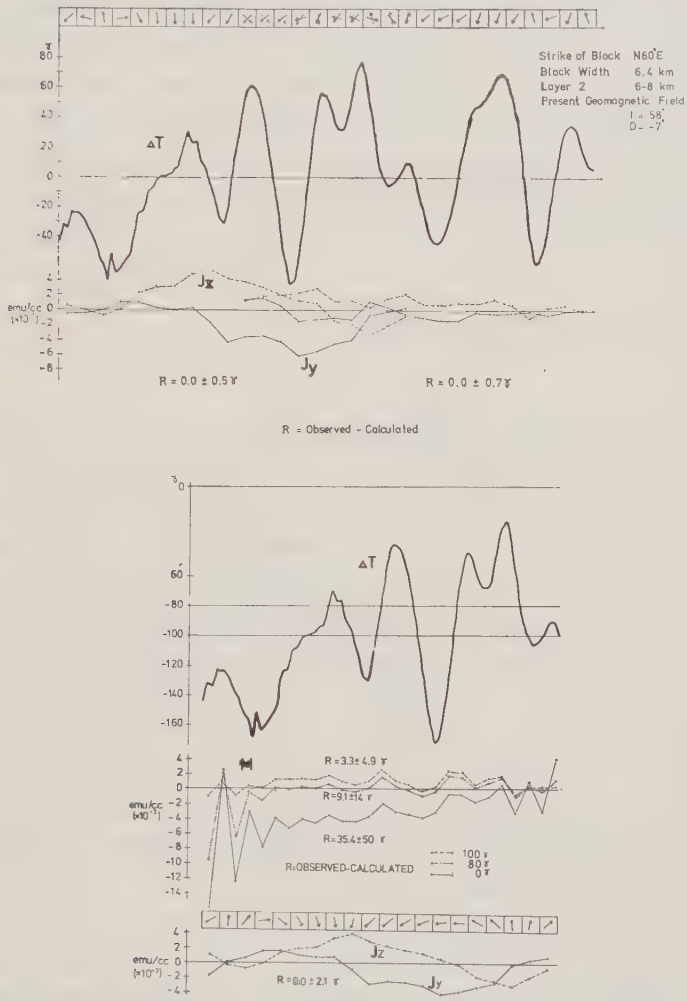

Fig. 31. Distribution of magnetization obtained under assumption of specified direction of magnetization in the Japan Sea. Three solutions correspond to three cases of shift of the zero level. Bottom diagram is the solution without the condition of specified direction of magnetization, in the case of the -80γ shift of the zero level.

diagram. In this case, the intensities range from 2.4×10^{-5} to 2.4×10^{-3} emu/cc which may suggest the rough topography of the surface of Layer 2 if it is uniformly magnetized.

Magnetizations of the dredged rocks from ocean bottom range from 10^{-4} emu/

cc to 10^{-3} emu/cc in magnitude except in the crestal region of the oceanic ridge (e. g. OZIMA et al., 1968, IRVING et al., 1970). Magnetizations of Layer 2 both in the northwestern Pacific and in the Japan Sea appear to be a little larger than those of rocks dredged from the sea floor in the non-specified direction model. If the magnetization of Layer 2 should have the same magnitude of magnetization as that of the dredged rocks, magnetization of the fixed direction parallel with the present earth's field (see Fig. 31) may be more plausible than the model in Fig. 30.

5. Tectonics of the Seas around Japan

5–1. Northwestern Pacific

In the sea floor spreading hypothesis, the lithosphere or the plate is created at the crest of a mid-oceanic ridge by intrusions of mantle derived material (magma). This meterial cools and solidifies at the surface as a thin veneer to form a new sea floor. The sea floor moves away from the crest of the ridge as more material is added at the ridge crest. As the magma cools it passes through its Curie temperature and becomes magnetized in the direction of the ambient geomagnetic field. The geomagnetic field is known to have repeated reversing its polarity at interval of the order of a million years since at least the late Cretanceous. These reversals build up, at the surface of the cooling magma, a pattern of oppositely polarized blocks distributed at different distances from the ridge crest. In turn these blocks produce discrete magnetic anomalies which imprint the reversal history of the main field and give rise to magnetic lineations parallel to the axis of the active spreading centers.

Near the crests of the ridge, the pattern of magnetic anomalies has been correlated with the known reversal time scale for the past 4 million years determined from land rocks and deep sea cores (e. g. COX et al., 1964). Further away from the crest, distinctive anomalies back to the early Cretaceous have been dated by comparison with the age of fossils recovered in the sediment cores of the JOIDES deep sea drilling program in the South Atlantic (MAXWELL et al., 1970). It appears from the land palaeomagnetic data that the frequency of reversals became much less during the middle Cretaceous (HELSLEY and STEINER, 1969). However, clear magnetic anomaly lineations—the Kiethly sequence—have been found in the western Atlantic (VOGT et al., 1971) and also in the western Pacific (HAYES and PITMAN, 1970). All of these regions are far from presently active ridge crests, and the age inferred from JOIDES cores appear to be older than the middle Cretaceous. Mag-

netic anomaly lineations in these regions seem to need fairly rapid reversals due to their apparent short wavelengths. On the other hand, there is landpalaeomagnetic evidence that there was a period of increased rate of reversals in the early Cretaceous-late Jurassic, 115–125 million years before present (MCELHINNY and BUREK, 1971). Combining these pieces of evidence, it may be reasonable to assume that the tectonics of the oceans dates back to the late Jurassic or earlier.

Possible correlations of magnetic anomaly lineations and their tectonic significance are considered by HIDE, SCLATER, ISEZAKI and WAGEMAN (1972).

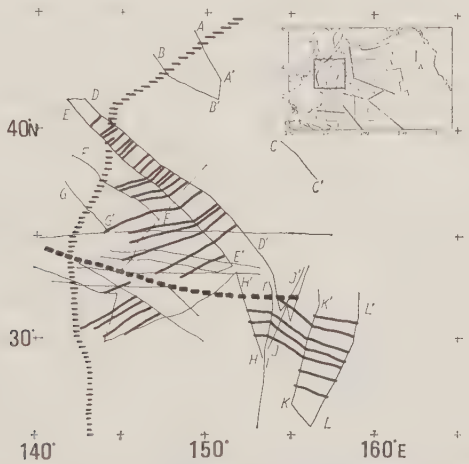

Fig. 32. Track lines concerned in this section. Magnetic anomaly lineations are also shown by thick solid lines.

On the basis of seven profiles of Fig. 32 in the region B in Fig. 12 a composite profile in the N45°E direction at 40°N was constructed as shown in Fig 33. This profile was compared with synthetic profiles generated from a block model. As it is possible that these northwestern Pacific anomalies would correspond to a part of the presently known magnetic time scale, an attempt was first made to match the anomalies to the synthetics generated for the older portion, anomalies 17 through 32, of the corrected HEIRIZLER et al. time scale (1968). The corrected older anomalies, 29 through 32, were taken from MCKENZIE and SCLALER (1971) (Fig. 34). Before making the match, three factors had to be taken into account. First, the direction of spreading in the area could be either N45°W or 180° out of it, i.e. S45°E. Secondly, the spreading rate could vary from 8 cm/yr to 2 cm/yr. Thirdly, the

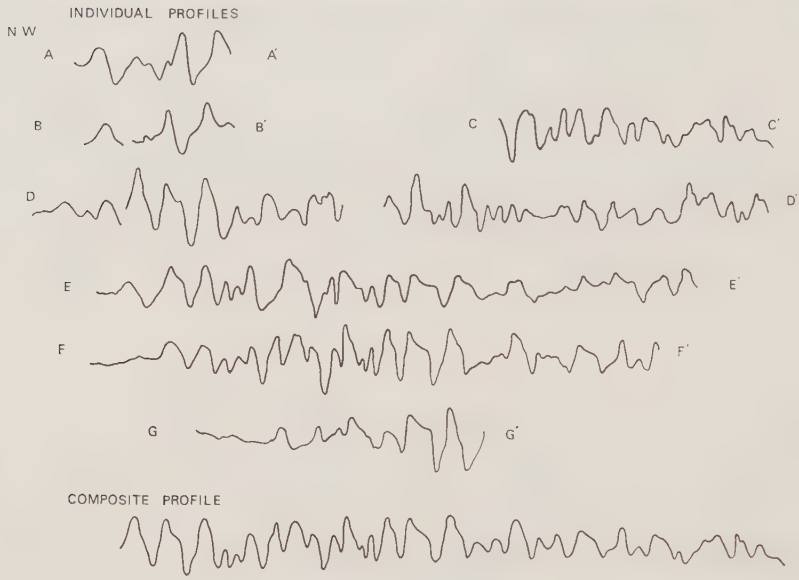

Fig. 33. Magnetic anomaly profiles in the northwestern Pacific, (See Fig. 32 for location of tracks).

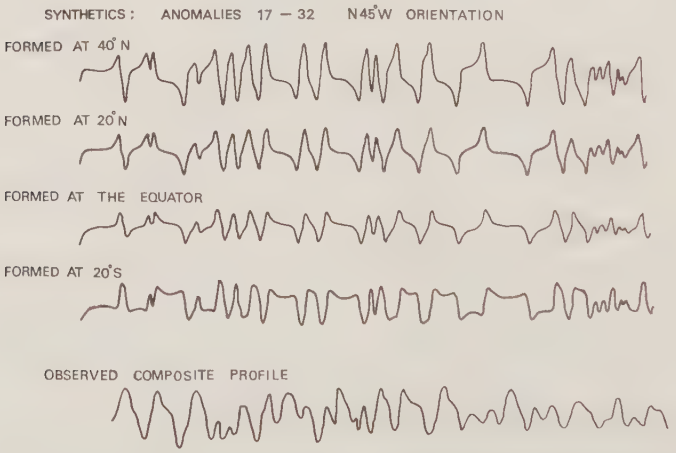
SYNTHETICS : ANOMALIES 17 — 32 N45°W ORIENTATION
FORMED AT 40° N
FORMED AT 20° N
FORMED AT THE EQUATOR
FORMED AT 20° S
OBSERVED COMPOSITE PROFILE

Fig. 34. Synthetic anomalies by the HEIRTZLERS' time scale and the observed composite profile.

anomalies, if they are old, could have easily been formed at a totally different latitude. The second factor is diffecult to control without producing great number of possible cases. In their study, an arbitrary spreading rate of 3 cm/yr was taken.

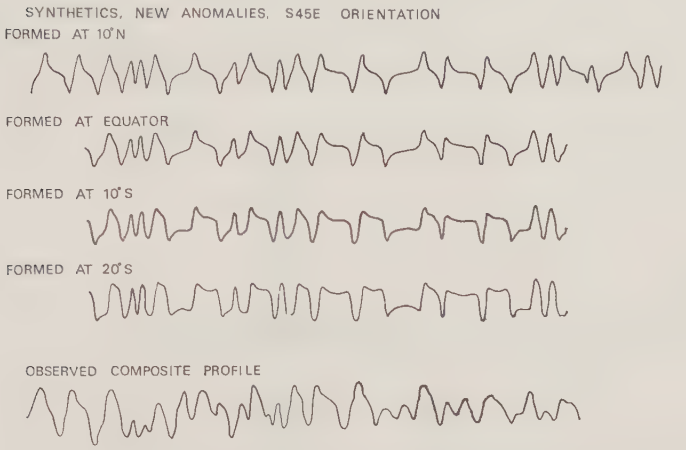

Fig. 35. Synthetic anomalies which fit best the observed composite anomalies, produced at the possible latitude of formation.

The third factor was taken into account by forming the blocks at different latitudes and observing them at 40°N. The results of comparison of observed composite profile and synthetics are shown in Fig. 35. As can be seen in this figure, there is no obvious relationship between the anomalies generated from the present time scale and the observed anomalies. It appears that the northwestern Pacific anomalies are not a part of the revised HEIRZLERS' time scale.

The next step was to make synthetic profiles from a block model. The model was constructed from the observed composite profile, but it was assumed to have been formed at different latitudes and observed at 40°N.

It is worth noticing in Fig. 35 that individual anomalies have a very definite asymmetry. They are more pronouncedly peaked on the NW side than on the SE side. Best match to the shape of the observed anomalies is given by synthetic profiles generated between the equator and 20°S. So it may be inferred that the crust of the whole region might have moved 40 to 50 degrees northwards since its formation. This inference agrees well with a shift of palaeolatitudes proposed from palaeomagnetism of seamounts in this area by UYEDA and RICHARDS (1965) and VACQUIER and UYEDA (1967).

HAYES and PITMAN (1970) reported the magnetic anomaly lineations trending NW–SE in the region around 25°N, 165°E, i. e. the south of Shatzky Rise. If there is a second magnetic bight (the first one is the "Great Magnetic Bight" in the northeastern Pacific) as suggested by HAYES and PITMAN (1970), the block model obtained from anomalies near Japan (Fig. 35) should match the model for the

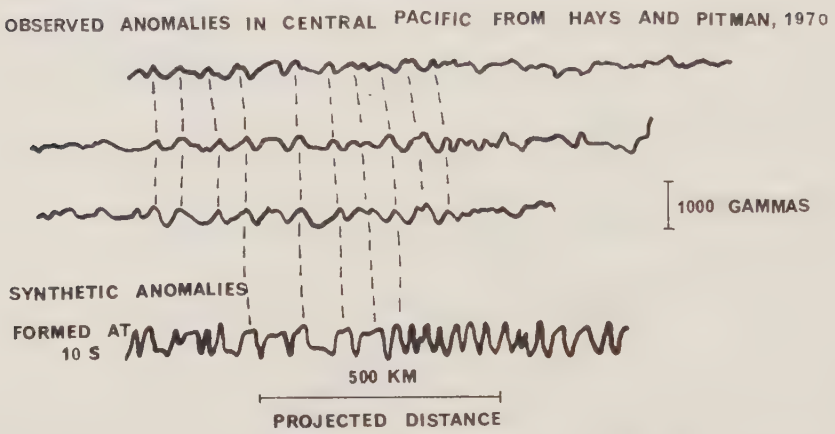

Fig. 36. Magnetic anomaly profiles south of the Shatzky Rise and the synthetic anomaly profile in the northwestern Pacific off Japan.

anomalies in the region around 25°N, 165°E by adjusting the spreading rate and the direction of blocks. HILDE, SCLATER, ISEZAKI and WAGEMAN (1972) further tested this hypothesis as shown in Fig, 36. The bottom profiled in Fig. 36 is the synthetic profile (formed at 10°S) rotated to N45°W, to be compared with the observed profiles (HAYES and PITMAN, 1970). Since a good match, though not dramatically convincing, is found for a spreading rate of 4/5 that near Japan, the hypothesis of a second magnetic bight may be fairly realistic.

The summary of the study of HILDE, SCLATER, ISEZAKI and WAGEMAN is as follows; the magnetic anomaly lineations in the northwestern Pacific near Japan are probably of an epoch older than that covered by the presently known magnetic timescale. Perhaps the age may be as old as the late Jurassic and the location where these lineations were formed was close to the equator. The best fit block model in the region gives a reasonable match to sections of magnetic anomaly lineations running NW–SE at around 25°N, 165°E. This may be taken as evidence that these anomalies have the same age as those which are found to their northwest near Japan and that there is a magnetic bight in the older anomalies in this area. The age is about Jurassic and increases in the direction of S45°E in the west side of the Emperor seamount chain, while in the east side, the age is about Cretaceous. So, the Emperor seamount chain or the Emperor Fracture Zone may be a kind of fault of which great horizontal displacement disconnects the magnetic anomaly lineations in either side of the Emperor seamount chain.

5–2. Japan Sea

Almost all the magnetic anomalies in the Japan Sea are, as mentioned in 3, negative by about −100 gammas. To explain these anomalies negative magnetiza-

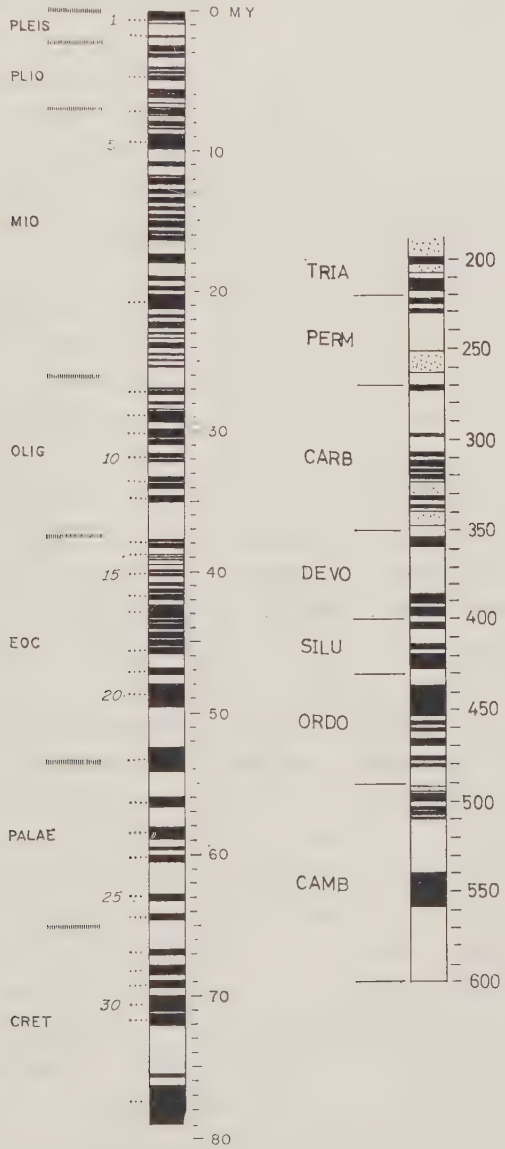

Fig. 37. The time scale of the reversal of the polarity of the earth's magnetic field by HEIRTZLER et al. (1968), and OZERSKAYA (1965).

tion of about 10^{-2} emu/cc in magnitude is needed. This implies that the floor of the Japan Sea might have been generated in the period of reversed polarity of the earth's field. After the time scale of reversals of the geomagnetic field by HEIRTZLER et al. (1968), a reversal period is about 1 million years long since the upper Cretaceous. If the evolution of the whole Japan Sea occurred within the duration of about 1 million years, we cannot determine which reverse epoch was the time of the evolution of the Japan Sea. If the duration of the evolution needed more than ten million years, it must go back to the Permian because it is believed that the geomagnetic field was predominantly normal from the Permian till the upper Cretaceous and in the time older than the Permian, the reverse periods were dominant (Fig, 38). (e. g. MCELHINNY, 1971).

The geological history of the Japan Sea is not known adequately but some geologists proposed their ideas on the genesis of the Japan Sea floor (e. g. FUJITA, 1963; GORAI et al., 1965; MURAUCHI, 1966; BERSENEV, 1971). According to these ideas the time of the beginning of the evolution or opening of the Japan Sea ranges from the Cretaceous (130 m. y.) to the middle Tertiary i. e. Oligocene (25～30 m. y.).

K–Ar age determinations give 197 and 200 m. y. for the ages of the granites dredged from the Kita-Yamato-Tai and the Nishi-Takuyo-Tai (SHIMAZU, 1968) and 4.16 to 21.6 m. y. for the ages of the basalts and andesites dredged from the Yamato-Tai and the seamounts near Honshu (UENO et al., 1971). But these data are insufficient to determine the definite age of the evolution of the Japan Sea.

Magnetizations obtained from the model calculation without assumption of fixed direction of magnetization yielded no abrupt changes of the directions even if the zero level of magnetic anomalies is changed as shown in Fig. 31. This may suggest that the magnetic structure of the Japan Sea floor is laterally rather homogeneous, while that of the northwestern Pacific is not. So it may be suggested that the evolution of the Japan Sea floor have occurred at one porality epoch. If the DC component of −100 gammas is assumed to be generated from sources underlying Layer 2, such as Layer 3 at 8 to 10 kms below the sea surface, the situation turns out to be a little different. In such a case, for instance, the negative magnetization of Layer 3 should be about 10^{-2} emu/cc and the AC components of magnetic anomalies fluctuating around the level of −100 gammas can be expalined in almost all the cases by positive magnetizations in Layer 2 ranging from, 8.8×10^{-4} to 4.5×10^{-3} emu/cc in magnitude as described in 4 (Fig. 31). In this case even a two stage-model of evolution might be imagined for the development of the Japan Sea, i. e. a reverse polarity epoch and the other at the normal polarity epoch.

Anyway, it appears that the tectonics in the Japan Sea resulted in the lateral homogeneity in the polarity of magnetization and the DC component of −100 gammas gives a slightly larger magnitude of magnetization than that of the northwestern Pacific (see 4). But it can be one order of magnitude less if DC component is generated in any other places than Layer 2.

6. Conclusions

The GSFC (12/66) field matches well the actual geomagnetic field in 1965 in and around Japan, except marginal seas such as the Japan and the Okhotsk Seas, but it does not in 1970 because of the poor quality of its secular change terms. As the secular change correction in and around Japan, the author obtained a value of −23 gammas/yr from the observed magnetic data.

The magnetization distribution obtained by solving a set of linear equations (4–2–8) without any restriction to the direction of magnetization presented features that are somewhat different from those of VINE and MATTHEWS hypothesis. If our analysis is more realistic, some corrections to the reversal time scale of the geomagnetic field by HEIRTZLER et al. (1968) may be called for.

In the northwestern Pacific, clear magnetic anomaly lineations are present, some of which need abrupt changes in the direction of magnetization. On the other hand, in the Japan Sea, the magnetic anomalies, though definitely elongated, have their amplitude about 1/5 and wavelength about 1/3 compared to those in the northwestern Pacific. It was shown that those anomalies do not need abrupt changes in the direction of magnetization. This implies that the tectonics of the northwestern Pacific could be discussed in terms of the sea-floor spreading or plate tectonics but that of the Japan Sea might be better discussed in terms of layered magnetization.

The age of the sea floor of the northwestern Pacific may be as old as the late Jurassic but that of the Japan Sea can not be determined from magnetic anomalies only.

The marginal seas in the western rim of the Pacific seem to have the DC component of about −100 gammas in their magnetic anomalies which might imply that the time of evolution of the marginal seas was the epoch(s) of the reverse polarity of the geomagnetic field.

Acknowledgements

The author thanks Prof. S. UYEDA for his substantial advices, critical reading

of the manuscript and continual encouragement throughout this study. He also thanks Prof. T. NAGATA and H. TAKEUCHI for their valuable suggestions. He thanks Prof. T. RIKITAKE, Prof. H. KANAMORI, Prof. M. YASUI and Assoc. Prof. T. YUKUTAKE for their helpful discussions and encouragement. The author is particularly grateful to Drs. T. W. C. HILDE, J. G. SCLATER and J. M. WAGEMAN for permitting him to include their joint work in this paper.

Collegues of the Prof. UYEDA's office, Dr. H. FUJISAWA for his help for operating a computer, Mr. T. WATANABE for his critical discussions and Miss N. MIZUSHIMA for drawing all figures and typing up this paper, are gratefully acknowledged.

Some magnetic surveys were carried out by partial finantial support by the grant (G–33) from Japan Society for Promotion of Science under the U. S.-Japan Science Cooperation Program.

References

ALLDREDGE, L.R. and G.D. VAN VOORHIS (1961): Depth to sources of magnetic anomalies. *J. Geophys. Res.*, **66**, 3793–3800.

ALLDREDGE, L.R., G.D. VAN VOORHIS and T.M. DAVIS (1963): A magnetic profile around the world. *J. Geophys. Res.*, **68**, 3679–3692.

ALLDREDGE, L.R. (1965): Analysis of long magnetic profiles. *J. Geomag. Geoele.*, **17**, 173–185.

BOTT, M.H.P. (1967): Solution of the linear inverse problem in magnetic interpretation with application to oceanic magnetic anomalies. *Geophys. J.*, **13**, 313–323.

BERSENEV, I.I. (1971): The origin of the Japan Sea basin. *Proc. First Japan-USSR Symposium on Solid Earth Sciences*, 31–37, (in Japanese).

BULLARD, E.C. (1967): The removal of trend from magnetic surveys. *Earth Planet. Sci. Letters*, **2**, 293–300.

CAIN, J.C., W.E. DANIELS and S.J. HENDRICKS (1965): An evaluation of the main geomagnetic field, 1940–1962. *J. Geophys. Res.*, **70**, 3647–3674.

CAIN, J.C., S.J. HENDRICKS, R.A. LANGEL and W.V, HUDSON (1967): A proposed model for the international geomagnetic reference field 1965. *J. Geomag. Geoel.*, **19**, 335–355.

COX, A., R.R. DOELL and G.B. DALRYMPLE (1964): Reversals of the Earth's magnetic field. *Science*, **144**, 1537–1543.

DICKSON, G.C., W.C. PITMAN, III, and J.R. HEIRTZLER (1968): Megnetic anomalies in the south Atlantic and ocean floor spreading. *J. Geophys. Res.*, **73**, 2087–2100.

DIETZ, R.S. (1961): Continental and ocean basin evolution by spreading of the sea floor. *Nature*, **190**, 854–857.

ELVERS, D.J., C.C. MATHEWSON, R.E. KOHLER and R.L. MORSES (1967): Systematic ocean surveys by the USC & CGS Pioneer 1961–1963. *ESSA Operation Data Report C & GS DR-1.*

EMILIA, D.A. and G. BODVARSSON (1969): Numerical methods in the direct interpretation of marine magnetic anomalies. *Earth Planet. Sci. Letters.*, **7**, 194–200.

ERICKSON, B.H. and P.J. GRIM (1969): Profiles of magnetic anomalies south of the Aleutian Island arc. *Geol. Soc. Amer. Bull.*, **80**, 1387–1390.

ERICKSON, B.H.: (private communication).

FANSELAU, G. and H. KAUTZLEVEN (1958): Die analytishe Darstellung des geomagnetishen Feldes. *Geofiscica Pura e Applicata*, **41**, 33–72.

FUJITA, S. (1963): When was the Japan Sea born? *Bull. Physical Geography Soc. Niigata*, **1**, 1–6, (in Japanese).

GRIM, P.J. and B.H. ERICKSON (1969): Fracture zones and magnetic anomalies south of the Aleutian Trench. *J. Geophys. Res.*, **74**, 1488–1499.

HAHN, A. (1965): Two applications of Fourier's analysis for the interpretation of geomagnetic anomalies. *J. Geomag. Geole.*, **17**, 195–225.

HASEBE, K., N. FUJII and S. UYEDA (1979): Thermal processes under island arcs. *Tectonophysics*, **10**, 335–355.

HAYES, D.E. and W.C. PITMAN, III: Magnetic lineations in the Northe Pacific (preprint).

HEIRTZLER, J.R. (1965): Marine geomagnetic anomalies. *J. Gemag. Geoele.*, **17**, 227–236.

HEIRTZLER, J.R., G.O. DICKSON, E.M. HERRON, W.C. PITMAN, III and X. LE PICHON (1968): Marine magnetic anomalies, geomagnetic field reversals and motions of the ocean floor and continents. *J. Geophys. Res.*, **73**, 2119–2163.

HELSLEY, C. and M.B. STEINER (1969): Evidence for long intervals of normal polarity during the Cretaceous period. *Earth Planet. Sci. Letters*, **5**, 325–332.

HESS, H.H. (1962): "History of ocean basins", in Petrogic Studies. A volume in Honor of A.F. BUDDINGTON, *Geol. Soc. Amer., New York*, 559–620.

HILDE, T.W.C., J.G. SCLATER, N. ISEZAKI and J.M. WAGEMAN: Magnetic anomalies in the northwestern Pacific, (in preparation).

HURWITZ, L., D.G. KNAPP, J.H. NELSON and D.E. WATSON (1966): Mathematical model of the geomagnetic field for 1965. *J. Geophys. Res.*, **71**, 2373–2383.

IAGA COMISSION 2 WORKING GROUP No. 4 Analysis of the geomagnetic field (1969): The international geomagnetic field 1965.0.

IRVING, E., W.A. ROBERTSON and F. AUMENTO (1969): The mid-Atlantic ridge near 45°N, IV. Remanent intensity, susceptibility and iron content of dredged samples. *Candian J. Earth Sci.*, **7**, 226–238.

IRVING, E., J.K. PARK, S.E. HAGGERTY, F. AUMENTO and B. LONCAREVIC (1970): Magnetism and opaque mineralogy of basalts from the mid-Atlantic Ridge at 45°N. *Nature*, **228**, 974–976.

ISEZAKI N. (1969): Magnetic anomalies at the seas around Japan. *Master Thesis, Graduate School Univ. of Tokyo.*

ISEZAKI, N. (1970): Magnetic anomalies at the seas around Japan. *Proc. Symposium on Thermal Structure under the Japan Islands*, 365–374, Akita Univ. (in Japanese).

ISEZAKI, N., K. HATA and S. UYEDA (1971): Magnetic survey of the Japan Sea, (Part 1). *Bull. Earthq. Res.*, **49**, 77–83.

ISEZAKI, N. and S. UYEDA (1972): Geomagnetic anomaly of the Japan Sea. Submitted to Phys. Earth Planet. Interiors.

ISEZAKI, N., M. YASUI and S. UYEDA: The seamount magnetisation in the Japan Sea (in preparation).

KARIG, D.E. (1970): Ridges and basins of the Tonga-Kermadec Island arc system. *J. Geophys. Res.*, **75**, 239–254.

KARIG, D.E. (1971): Origin and development of marginal basins in the western Pacific. *J. Geophys. Res.*, **76**, 2542–2560.

LEATON, B.R., S.R.C. MALIN and M.J. EVANS (1965): An analytical representation of estimated geomagnetic field and its secular change for the epoch 1965.0. *J. Geomag. Geoele.*, **17**, 187–194.

LELICHON, X. and J.R. HEIRTZLER (1968): Magnetic anomalies in the Indian Ocean and sea-floor spreading. *J. Geophys. Res.* **73**, 2101–2117.

LUDWIG, W.J., J.I. EWING, M. EWING, S. MURAUCHI, N. DEN, S. ASANO, H. HOTTA, M. HAYAKAWA, T. ASANUMA, K. ICHIKAWA and I. NOGUCHI (1966): Sediments and structure of the Japan Trench. *J. Geophys. Res.*, **71**, 2121–2137.

MASON, R.G. (1958): A magnetic survey off the west coast of the United States between Latitude 32° and 36°N, Longitude 121° and 128°W, *Geophys. J.*, **1**, 320–329.

MASON, R.G. and A.D. RAFF (1961): A magnetic survey off the west coast of north America, 32°N to 42°N. *Geol. Soc. Amer. Bull.*, **72**, 1249–1265.

MATSUDA, T. and S. UYEDA (1971): On the Pacific-type orogeny and its model-extension of the paired belts concept and possible origin of marginal sea. *Tectonophysics*, **11**, 5–27.

MATSUZAKI, T. (1968): Magnetic survey of Japan; 1962–1965. *Technical Report of Hydrographic Office, Tokyo*, **1**.

MAXWELL, A.E., R.P. VON HERZEN, K. JINGHWA HSU, I.E. ANDREWS, T. SAITO, S.F. PERCIVAL, Jr., E.D. MILOW and R.E. BOYCE (1970): Deep Sea drilling in the south Atlantic. *Science*, **168**, 1047–1059.

MCELHINNY, M.W. and P.J. BUREK (1971): Mesozoic palaeomagnetic stratigraphy. *Nature*, **232**, 98–102.

MINATO, M., M. GORAI and M. FUNAHASHI (1965): *The geologic development of the Japanese Islands.* Tsukiji Shokan, Tokyo.

MORGAN, W.J. (1968): Risese, trenches, great faults and crustal blocks. *J. Geophys. Res.*, **73**, 1959–1982.

MURAUCHI, S. (1966): Origin of the Japanese Islands. *Seien*, March, 20–23, (in Japanese).

MURAUCHI, S., T. ASANUMA and H. ISHII (1973): Geophysical studies in the seas around Hokkaido. *Memoir Nat. Sci. Museum*, **No. 6**, (in printting).

NAGATA, T. (1938): Magnetic anomalies and corresponding subterranean mass distribution. *Bull. Earthq. Res. Inst.*, **14**, 550–577.

NAGATA, T. and T. OGUTI (1962): Magnetic charts for the epoch of 1958.5 corrected for the Antarctic region and spherical harmocic coefficients of the revised geomagnetic field. *J. Geomag. Geoele.*, **14**, 125–131.

OPDYKE, N.D., B. GLASS, J.D. HAYS and J. FOSTER (1966): Palaeomagnetic study of Antarctic deep-sea cores. *Science*, **154**, 349–357.

OZIMA, M., M. OZIMA and I. KANEOKA (1968): Potassium-argon ages of some dredged submarine basalts and their geophysical implications. *J. Geophys. Res.*, **73**, 711–723.

PETER, G., B.H. ERICKSON and P.J. GRIM (1970): Magnetic structure of the Aleutian Trench and northeast Pacific basin. *The Sea*, **Vol. 4**, Edited by A.E. MAXWELL, 191–222, Wiley-Interscience, New York.

PITMAN, W.C. III, E.M. HERRON and J.R. HEIRTZLER (1968): Magnetic anomalies in the Pacific and se-floor spreading. *J. Geophys. Res.*, **73**, 6069–2085.

RAFF, A.D. and R.G. MASON (1961): Magnetic survey off the west coast of North America, 40°N to 52.5°N. *Bull. Geol. Soc. Amer.*, **72**, 1259–1265.

Report on Aeromagnetic Survey in Japan, World Data Center C2 for Geomagnetism, 1966.

RIKITAKE, T., S. MIYAMURA, I. TSUBOKAWA, S. MURAUCHI, S. UYEDA, H. KUNO and M. GORAI (1968): Geophysical and geological data in and around the Japan Arc. *Canadian J. Earth Sci.*, **5**, 1101–1118.

SEGAWA, J. (1967): A method of determining subterranean anomalous structure from the distribution of local anomaly in geomagnetic total force. *J. Geood. Soc. Japan*, **13**, 20–44.

SHIMAZU, M. (1968: On the absolute age of granites of Yamato-tai. *The Japan Sea*, **2**, 55–

68, Kanazawa Univ., (in Japanese).

Solov'yev, O.N. and A.G. Gainanov (1963): Geological structure in the zone of transition from the Asiatic continent to the Pacific Ocean in the region of the Kuril-Kamchatka Island arc. *Soviet Geol.*, **3**, 113–123.

Talwani, M. (1965): Computation with the help of a digital computer of magnetic anomalies caused by bodies of arbitrary shape. *Geophysics*, **30**, 797–817.

Talwani, M., C.C. Windish and M.G. Langseth, Jr. (1971): Reykjanes Ridge crest: A detailed geophysical study. *J. Geophys. Res.*, **76**, 473–517.

Ueno, N., I. Kaneoka, M. Ozima, T. Zashu, T. Sato and Y. Iwabuchi (1970): K-Ar age, Sr isotropic ratio and K/Rb ratio of the volcalic rocks dredged from Japan Sea. *Proc. First Japan-USSR Symposium on Solid Earth Sciences*, 305–309, (in Japanese).

Uyeda, S., M. Yasui, K. Horai and T. Yabe (1962): Report on geomagnetic during JEDS-4 Cruise. *Oceanogr. Mag.*, **13**, 167–183.

Uyeda, S., V. Vacquier, M. Yasui, J. Sclater, T. Sato, J. Lawson, T. Watanabe, F. Dixon, E. Silver, Y. Fukao K. Sudo, M. Nishikawa and T. Tanaka (1967): Results of geomagnetic survey during the cruise of R/V Argo in western Pacific 1966 and the compilation of magnetic charts of the same area. *Bull. Earthq. Res. Inst.*, **45**, 799–814.

Uyeda, S. and M. Richards (1966): Magnetization of four Pacific seamounts near the Japanese Islands. *Bull. Earthq. Res. Inst.*, **44**, 179–213.

Uyeda, S. and V. Vacquier (1968): Geothermal and geomagnetic data in and around the island arc of Japan. in The Crust and Upper Mantle of the Pacific Area, edited by L. Knopoff, C. Drake and P. Hart, *Geophysical Monogr.*, **No. 12**, 349–366, American Geophys. Union.

Uyeda, S. and A. Sugimura (1972): Island arcs. Elsevier, Amsterdam (preprint).

Vacquier, V., A.D. Raff and R.E. Warren (1961): Horizontal displacement in the floor of the Pacific Ocean. *Bull. Geol. Soc. Amer.*, **72**, 1267–1270.

Vacquier, V. (1963): A machine method for computing the magnitude and the direction of magnetization of a uniformaly magnetized body from its shape and a magnetic survey. *Proc. Benedum Earth Magnetism Sympesium 1962*, 123–137, Univ. Pittsburg Press.

Vestine, E.H., W.L. Sibley, J.W. Kern and J.L. Carlstadt (1963): Integral and spherical harmonic analysis of the geomagnetic field for 1955.0, Part-1. *J. Geomag. Geole.*, **15**, 47–72.

Vine, F.J. and D.H. Mathews (1963): Magnetic anomalies over oceanic ridges. *Nature*, **199**, 947–949.

Vine, F.J. and J.T. Wilson (1965): Magnetic anomalies over a young oceanic ridge off Vancouver Island. *Science*, **150**, 485–489.

Vine, F.J. (1966): Spreading of the ocean floor: New evidence. *Science*, **154**, 1405–1415.

Vogt, P.V., C.N. Anderson and D.R. Bracy (1971): Mesozoic magnetic anomalies, Sea-floor spreading and geomagnetic reversals in the southwestern north Atlantic. *J. Geophys. Res.*, **76**, 4796–4823.

Wageman, J.M., T.W.C. Hilde and K.O. Emery (1970): Structural framework of East China Sea and Yellow Sea. *The Amer. Asoc. Petr. Geol. Bull.*, **54**, 1611–1643.

Wilson, J.T. (1965): A new class of faults and their bearing on continental drift. *Nature*, **207**, 343–345.

Yasui, M., Y. Hashimoto and S. Uyeda (1967): Geomagnetic and bathymetric study of the Okhotsk Sea (1), *Oceanogr. Mag.*, **19**, 73–85.

Yasui, M.Y. Hashimoto and S. Uyeda (1967): Geomagnetic studies of the Japan Sea—Anomaly pattern in the Japan Sea—. *Oceanogr. Mag.*, **19**, 221–231.

The Oceanographical Magazine, Vol. 24, No. 2 (1973)

YASUI, M., K. NAGASAKA, Y. HASHIMOTO and K. ANMA (1968): Geomagnetic and bathymetric study of the Okhotsk Sea (2). *Oceanogr. Mag.*, **20**, 65–72.

日本列島周辺海域の地磁気異常と構造

伊勢崎　修弘

（気象大学校）

日本近海で観測された地磁気全磁力の現存全資料を GSFC (12/66) (Godard Space Flight Center) を使用して調査をしなおした。GSFC (12/66) は 1965 年現在のこ海域の観測地磁気場と良く合っているが，永年変化に関する項の精度が不充分で，1965年以降の観測値との差は年を追うに従って大きくなってゆくので，観測値と比較する際には GSFC (12/66) に $-25\,\gamma$/yr の永年変化補正を行った。

本州東方の北西太平洋では，振幅（山から谷までの値）500 乃至 1,000 γ，波長 50 乃至 80 km の縞状地磁気異常が認められたが，異常の縞模様と直交する方向の断面分布は，現在知られている地球磁場反転の歴史から計算されたものと良い類似を示す他のいずれの海域の断面分布とも対応せず，生成年代の推定はできなかった。しかし，異常の断面分布の型からは，赤道から南緯 10° までの間の海域で形成・帯磁されたものが現位置まで移動したことを示しており，古地磁気学的研究から提唱されている，この海域にある海山が緯度で 30° に及ぶ北方漂移をしたとする説を支持している。またこの海域の海底が元の位置で生成された時の拡大の方向と速度とを適当に変えて海面で観測される筈の異常の断面分布を計算してみると，シャッキー・ライズの南側の海域の東西方向の縞状異常の断面分布に一致させることができる。この南北隣接海域の縞状異常がいずれも後期ジュラ紀の地球磁場の反転が頻に繁起ったことに起因するものとすると，この両海域の境界部には Magnetic bight があって然るべきである。北西太平洋の構造を解明してゆく上から，一層充実した地磁気調査を行う必要がある。

一方，日本海にも日本列島に平行した方向性をもつ地磁気異常が認められるが，細長い斑を連ねたような模様で縞状とは言い難く，振幅で 200 γ 以下で波長も精々 40 km と短かい。このような地磁気異常の様相は一連の縁海，例えばオホーツク海，黄海，東シナ海などに共通のもののようである。このような特徴は縁海の構造が，典型的な海の構造と全く異ることを示すものと言えよう。

地磁気異常の解析結果をそのままに解釈すると，日本海の地磁気異常はは日本海全域にわたる一様な帯磁によって起こされたものであり，一方北西太平洋側の地磁気異常は帯磁方向が急変することによって起こされたものと言える。また地磁気異常の正負は必ずしも直下の構造中の帯磁方向の正逆とは対応しないことをも物語っている。

気象庁

欧文海洋報告

第 24 巻

THE OCEANOGRAPHICAL MAGAZINE

Vol. 24

Published by the Japan Meteorological Agency

March, 1973

CONTENTS

MORIYASU, S.: On short-term fluctuations of the Tsushima Current to the northwest of the Noto Peninsula in October 1969 1

NAGASAKA, K. and T. SAWARA: A preliminary report of the cruise of the R/V *Ryofu Maru* in January-March 1971 25

IIDA, H.: Edge waves on the linearly sloping coast II. Forced waves and β-effect 39

AKAGAWA, M.: The mean sea surface temperature of the Okhotsk Sea in cooling season (Second report) ——Normal sea surface temperature—— .. 57

YOSHIMURA, H.: On the distribution of phosphorus along 170°W longitude in the Pacific and Antarctic Oceans 65

AKAGAWA, M.: The characters of atmospheric circulation in the years with abnormal sea ice conditions along the Okhotsk coast of Hokkaido, Japan 81

DEN, N. and M. YASUI: A note on the palaeogeographic location of trenches ..101

ISEZAKI, N.: Geomagnetic anomalies and tectonics around the Japanese Islands 107

昭和48年3月31日　発行

編集兼
発行者　気象庁
東京都千代田区大手町1の3の4

印刷者　藤原秀雄

印刷所　昌美印刷株式会社
東京都千代田区神田錦町3の16